



**TECHNISCHE
UNIVERSITÄT
WIEN**
Vienna University of Technology

DIPLOMARBEIT

“Neutron Activation Analysis Measurement in Different Energy Ranges at the TRIGA Mark II Reactor for Determination of the Neutron Spectrum”

Ausgeführt am
Atominstitut der Technischen Universität Wien

unter der Anleitung von
Ao.Univ.Prof.i.R. Projektass. Dipl.-Ing. Dr.techn. Helmuth Böck,
Senior Scientist Dipl.-Ing. Dr.techn. Mario Villa
und
Marcella Cagnazzo, M.Sc.

durch

Christina Raith, B.Sc.
Gumpendorfer Straße 69
1060 Wien

Wien, Mai 2015

(Christina Raith)

Abstract

Essentially, this master thesis represents the experimental facet of the evaluation of a reactor neutron spectrum. In the course of the work conducted, neutron activation analysis measurements were performed at the TRIGA Mark II reactor at the Atominstitut of the Vienna University of Technology. The data obtained was used for an ongoing research project at the Atominstitut related to the neutron flux characterisation for the new core.

The work included the selection of activation foils that would meet the requirements, the design of sample holders for different irradiation positions – in particular a horizontal beam tube and the central irradiation channel – as well as the planning and performing of irradiations and gamma spectroscopy measurements of activated foils.

The activation foils that were used in the course of this work were chosen with regard to the pureness of the material and geometry considerations. The materials were gold, copper, indium, nickel, iron and aluminium. The reactions that were of essential for covering the entire neutron energy spectrum included (n,γ) , (n,n') and (n,p) reactions, some of which exhibited threshold behaviour. The half-lives of the activation products were quite diverse, ranging from a few minutes, in the case of ^{27}Mg , to almost a year in the case of ^{54}Mn . The gamma spectroscopy measurements were performed in such a way as to minimize the statistical and systematic uncertainties.

The irradiations were planned in order to achieve an optimal activation of the foils but within reasonable limitations such as radiological protection and time constraints. In the horizontal beam tube, irradiations were performed in three different positions along the horizontal axis of the tube. The collimator had been removed before these measurements. For irradiations in the central irradiation channel, a special sample holder, which allowed the irradiation of foils in eleven positions along the vertical axis, was designed. Since the irradiations were performed at different times and under varying circumstances, there was also an extra reference position for flux monitoring in the sample holder.

The irradiations and measurements that were performed were overall very satisfying and provided useful data, which could subsequently be used for further research.

Zusammenfassung

Diese Diplomarbeit basiert auf dem Prinzip der Neutronenaktivierungsanalyse. Im Zuge der Arbeit wurden Metallfolien durch Bestrahlung am TRIGA Mark II Reaktor des Atominstututs der Technischen Universität Wien aktiviert und mittels Gammaskopie ausgewertet. Die dadurch gewonnenen Daten wurden für ein laufendes Forschungsprojekt zur Charakterisierung des Neutronenflusses im neuen Reaktorkern des TRIGA Mark II Reaktors des Atominstututs verwertet.

Die grundsätzlichen Bestandteile dieser Arbeit umfassten die Auswahl geeigneter Folien, das Entwerfen von Probenhaltern für diverse Bestrahlungseinrichtungen – im Speziellen handelte es sich hierbei um ein radiales Strahlrohr und das zentrale Bestrahlungsrohr in der Mitte des Reaktorkernes– die Planung und Durchführung der Bestrahlungen, sowie Gammaskopie der aktivierten Proben.

Die zu bestrahlenden Folien bestanden aus den Materialien Gold, Kupfer, Indium, Nickel, Eisen und Aluminium. Sie wurden in Hinblick auf ihre Reinheit sowie Geometrie ausgewählt. Bei den Reaktionen, die nachgewiesen werden sollten, handelte es sich um (n,γ) , (n,n') und (n,p) Reaktionen, wobei einige davon durch eine gewisse Schwellenenergie der Aktivierung charakterisiert wurden. Die Halbwertszeiten der Aktivierungsprodukte waren stark unterschiedlich und schwankten zwischen einigen Minuten auf der einen Seite und fast einem Jahr auf der anderen Seite. Die Messungen wurden daher für die einzelnen Folien so variiert und an die Bedingungen angepasst, dass die statistischen und systematischen Unsicherheiten minimiert werden konnten.

Die Bestrahlungen wurden derart geplant und durchgeführt, dass trotz der Einschränkungen in Bezug auf Reaktorverfügbarkeit und Strahlenschutz eine optimale Aktivierung der Folien gewährleistet werden konnte. Im radialen Strahlrohr wurden drei verschiedenen Positionen entlang der horizontalen Achse des Strahlrohres charakterisiert. Für die Bestrahlungen im zentralen Bestrahlungsrohr wurden spezielle Probenhalter konstruiert. Diese ermöglichten die Bestrahlung von Folien in elf verschiedenen Positionen entlang der vertikalen Achse. Zusätzlich war auch eine Referenzposition zur Überwachung des Neutronenflusses inkludiert.

Die durchgeführten Bestrahlungen und Messungen lieferten äußerst zufriedenstellende Resultate und konnten für weiterführende Berechnungen und Forschungen herangezogen werden.

Acknowledgements

I would like to express my gratitude to my supervisors Marcella Cagnazzo, M.Sc., Senior Scientist Dipl.-Ing. Dr.techn. Mario Villa and Ao.Univ.Prof.i.R. Projektass. Dipl.-Ing. Dr.techn. Helmuth Böck. They guided me throughout the experimental work as well as the writing process of this master thesis and I am very grateful for their patience, dedication and support. In addition, I would like to thank the other employees of the Atominstitut, in particular the radiation protection group, for the use of their equipment and their continual assistance and advice. On a final note, I would like to thank my loved ones for their never ending support and encouragement.

Contents

I Fundamentals

1 Nuclear Basics	3
1.1 Atomic Structure	3
1.2 Atomic Mass and Energy	4
1.3 Binding Energy and Mass Defect	5
2 Radioactive Decay and Radiation Physics	7
2.1 Types of Radioactive Decay	7
2.1.1 Alpha Decay	7
2.1.2 Beta Decay	8
2.1.3 Internal Conversion	11
2.1.4 Neutron or Proton Emission	11
2.1.5 Spontaneous Fission (SF) and Neutron-Induced Fission	11
2.1.6 Electromagnetic Radiation	12
2.2 Activity and Decay Law	14
2.3 Decay Chains	16
2.4 Interaction of Electromagnetic Radiation with Matter	17
2.4.1 Photoelectric Effect	17
2.4.2 Compton Effect	17
2.4.3 Pair Production	18
2.4.4 Attenuation	18
3 Nuclear Reactions	19
3.1 Reaction Types	19
3.2 Q-value of a Reaction	20
3.3 Reaction Cross Section	20
3.3.1 Partial and Total Cross Section	21
4 A Nuclear Reactor as a Neutron Source	23
4.1 The Configuration of a Nuclear Fission Reactor	23
4.2 Reactor Neutron Energy Spectrum	24

5	Radiation Detection	27
5.1	Basic Principle	27
5.2	General Terms	27
6	Counting Statistics	29
6.1	The Binominal Distribution	29
6.2	The Poisson Distribution	30
6.3	The Gaussian Distribution	30
7	Radiation Protection and Dose Rates	31
7.1	The Principles of Radiological Protection	31
7.2	Biological Effects	32
7.3	Dose Quantities	33
7.3.1	Absorbed Dose	33
7.3.2	Equivalent Dose	33
7.3.3	Effective Dose	34
 II Methods and Materials		
8	Neutron Activation Analysis	37
8.1	Principle of Neutron Activation Analysis (NAA)	37
8.2	Foil Activation for Determination of the Neutron Flux	39
9	The TRIGA Mark II Reactor	43
10	Data Analysis: Gamma Spectroscopy - Detector and Software	47
10.1	Basics of Semiconductor Detectors	47
10.1.1	Basic Principle of Semiconductors	47
10.1.2	Semiconductor Detectors	48
10.1.3	Germanium Detectors	50
10.2	Gamma Spectroscopy	50
11	Laboratory Equipment	51
11.1	Detector	51
11.2	Software	53
11.3	Calibration	53
11.3.1	Energy Calibration	53
11.3.2	Efficiency Calibration	54
12	Experimental	59
12.1	Reactions	59
12.2	Foils	64

12.3 Irradiations	67
12.3.1 Horizontal Beam Tube	67
12.3.2 Central Irradiation Channel	69
12.4 Reactor Power Calibration	73
III Data Analysis and Conclusion	
13 Data Analysis and Results	79
13.1 Calculations	79
13.2 Beam Tube - Results	81
13.3 Central Irradiation Channel - Results	83
14 Conclusion	93
15 Bibliography	95
IV Appendix	
A Detector Data Sheet	101
B Calibration Source	103
C Foil Certificates	107
D Blueprints of the Vertical Cross Section of the Reactor	115

List of Figures

1.1	Binding energy per nucleon	6
2.1	Alpha decay of ^{238}U	8
2.2	General β -particle energy spectrum	10
2.3	Illustration of the decay law	16
3.1	Reaction target area	21
3.2	Reaction cross section of ^{197}Au	22
4.1	A typical reactor neutron energy spectrum	24
8.1	Major decay channels for $^{28}\text{Al}^*$	38
8.2	Absorption cross section of cadmium	41
9.1	Illustration of a fuel element	44
9.2	Vertical section of the TRIGA Mark II reactor	45
9.3	Horizontal section of the TRIGA Mark II reactor	45
9.4	Illustration of the core configuration	46
10.1	Illustration of the energy band structure of different materials	48
10.2	Schematic display of the atomic lattice of a doped tetravalent semiconductor	48
10.3	Basic configuration of a semiconductor junction	49
11.1	Gamma detector with additional shielding and liquid nitrogen cooling	52
11.2	Inside of the gamma detector in a typical measurement configuration	52
11.3	Energy calibration curve for the small measuring table	55
11.4	Efficiency calibration curve for the small measuring table (linear scale)	55
11.5	Efficiency calibration curve for the small measuring table (logarithmic scale)	56
11.6	Energy calibration curve for the medium measuring table	56
11.7	Efficiency calibration curve for the medium measuring table (linear scale)	56
11.8	Efficiency calibration curve for the medium measuring table (logarithmic scale)	57
12.1	Typical gamma spectrum of an activated gold foil	60
12.2	Decay scheme of ^{198}Au	60
12.3	Decay scheme of ^{64}Cu	61
12.4	Decay scheme of $^{115}\text{In}^*$	62

List of Figures

12.5	Decay scheme of ^{58}Co	62
12.6	Decay scheme of ^{54}Mn	63
12.7	Decay scheme of ^{27}Mg	63
12.8	Cadmium cut-off energy as a function of the cadmium thickness	65
12.9	Cadmium covers	66
12.10	Irradiation positions in the horizontal beam tube	68
12.11	Sample holder used for irradiations in the horizontal beam tube	68
12.12	Sample holder with close-up view of the suspended foils	69
12.13	Determination of the central core position	71
12.14	Aluminium sample holder	72
12.15	Sample holder made of MAKROLON [®]	72
12.16	Illustration of the linearity of the saturated activity	75
13.1	Saturated activities as a function of distance from the reflector	82
13.2	Saturated activity of gold foils	84
13.3	Saturated activity of cadmium-covered gold foils	85
13.4	Saturated activity of copper foils	86
13.5	Saturated activity of cadmium-covered indium foils	87
13.6	Saturated activity of nickel foils	88
13.7	Saturated activity of iron foils	89
13.8	Saturated activity of aluminium foils	90

List of Tables

11.1	Characteristics of the detector used in the course of this work	51
11.2	Nuclides and their photo peak energies contained in the certified calibration source	54
12.1	List of nuclides and information about the reactions	59
12.2	Information about the activation foils used in this work	64
12.3	Irradiations performed in the horizontal beam tube	70
12.4	Irradiations conducted in the central irradiation channel	73
13.1	Important constants concerning activation foils	80
13.2	Reactions, half-lives and decay constants for calculations	80
13.3	Saturated activities for the irradiations in the beam tube positions	82
13.4	Evaluation of the reference foils from the central irradiation channel	83
13.5	Central irradiation channel: results for gold foils	84
13.6	Central irradiation channel: results for cadmium-covered gold foils	85
13.7	Central irradiation channel: results for copper foils	86
13.8	Central irradiation channel: results for cadmium-covered indium foils	87
13.9	Central irradiation channel: results for nickel foils	88
13.10	Central irradiation channel: results for iron foils	89
13.11	Central irradiation channel: results for aluminium foils	90

Part I

Fundamentals

1 Nuclear Basics

1.1 Atomic Structure

An atom consists of electrons, protons and neutrons. An atom is roughly 10^{-10} m in diameter and consists of a positively charged core and a negative electron shell. The atomic core, the so-called nucleus, is only 10^{-14} m in diameter but contains most of the mass. The nucleus consists of protons and neutrons which are called nucleons correspondingly. The mass of a proton and a neutron is very similar, in the order of 10^{-27} kg. An electron is much lighter with a mass in the order of 10^{-31} kg. [?, p.9] [?, p.69]

Since protons have a positive elementary charge (elementary charge $e_0 = 1.602 \cdot 10^{-19}$ C) and neutrons are uncharged, the nucleus is positively charged. Electrons have a negative elementary charge. Thus, the positive charge of the atomic core is compensated by the negatively charged electron shell. If the number of protons is equal to the number of electrons, the whole atom is neutral which means it has no charge. If an atom has more protons in the core than electrons in the shell, it is positively charged which is also called ionised. [?, p.9f]

It is important to note, that a neutron is only stable when confined within an atomic core. The reason for this is its high binding energy. As a free particle a neutron is not stable and decays with a mean lifetime of approximately 15 min into a proton, an electron and an antineutrino. [?, p.9] [?, p.37]

The components of a nucleus can be described by the following simple equation:

$$A = N + Z \tag{1.1}$$

where A is the so-called mass number or nucleon number, N is the number of neutrons and Z is the proton number, which is also called the atomic number.

A certain species of an atom is called nuclide and is characterised by a defined number of protons and neutrons. The most accurate way to characterise a certain nuclide of the chemical element X is in the form of:

$${}^A_Z X_N \tag{1.2}$$

In this notation all the relevant numbers Z , N and A are specified. For example ${}^{13}_6 C_7$ refers

to a carbon nuclide with 6 protons and 7 neutrons and therefore a mass number of 14. Since a chemical element is identified by the proton number anyhow, there is another short notation in the form of ${}^A X$ or to avoid the superscript in the form of X-A. Using the prior example of ${}^{13}_6 C_7$, one could also write ${}^{13}C$ or C-13 to specify that same nuclide. [?, p.69] [?, p.10] [?, p.14]

There are around 270 stable nuclides, and over 3000 radioactive nuclides, so-called radionuclides, which either exist naturally on Earth or can be produced artificially. An organized overview over this vast number of nuclides is provided by a nuclide chart, where the number of protons is plotted over the number of neutrons. Also other important properties are provided in such charts, for instance information about the radioactive decay. Probably the most widely used nuclide chart is the Karlsruhe nuclide chart, see [?]. [?, p.13] [?, p.10]

As mentioned above, the number of protons defines a particular element, for example carbon has a proton number of 6. Atoms with the same number of protons but different mass numbers are called isotopes. Every chemical element has more than one not necessarily stable isotope. For instance carbon has five isotopes, which are ${}^{10}_6 C$, ${}^{11}_6 C$, ${}^{12}_6 C$, ${}^{13}_6 C$, and ${}^{14}_6 C$, of which only ${}^{12}_6 C$ and ${}^{13}_6 C$ are stable. The other isotopes are radioactive and are called radioisotopes consequently. For a particular element there is a certain fixed ratio of the naturally occurring and mostly stable isotopes which is called the isotopic abundance. For instance natural carbon is comprised of 98.90% ${}^{12}_6 C$ and 1.10% ${}^{13}_6 C$. [?, p.69] [?, p.14]

1.2 Atomic Mass and Energy

Einstein's equation describes the conversion of mass to energy which is necessary for most calculations concerning nuclear energies. For particles with non-relativistic velocities the equation is:

$$E = m \cdot c_0^2 \tag{1.3}$$

where E is the energy in joule, m is the rest mass in kilogram and c_0 is the vacuum speed of light, which is $c_0 = 2.9979 \cdot 10^8$ m/s.

Since 1 J is very large on a nuclear scale, the more commonly used energy unit is the electron volt (eV). It is defined as the kinetic energy an electron gains when passing through a potential difference of 1 V. The conversion of those two units is:

$$1 \text{ eV} = 1.6022 \cdot 10^{-19} \text{ J} \tag{1.4}$$

Since the nuclear masses are also very small on the large SI unit scale of kilogram, the atomic mass unit u (or AMU) has been defined to make calculations and comparisons more convenient. The atomic mass unit is defined as one twelfth of the mass of a neutral ${}^{12}C$

atom:

$$1 \text{ u} = \frac{m(^{12}\text{C})}{12} = 1.66054 \cdot 10^{-27} \text{ kg} = 931.5 \text{ MeV} \quad (1.5)$$

The rest masses of the neutron, proton and electron in the various units can be found below. [?, p.3] [?, p.14f] [?, p.12]

- Neutron: $m_n = 1.6749 \cdot 10^{-27} \text{ kg} = 1.0087 \text{ u} = 939.565 \text{ MeV}$
- Proton: $m_p = 1.6726 \cdot 10^{-27} \text{ kg} = 1.0073 \text{ u} = 938.271 \text{ MeV}$
- Electron: $m_e = 9.1094 \cdot 10^{-31} \text{ kg} = 5.4858 \cdot 10^{-4} \text{ u} = 0.511 \text{ MeV}$

1.3 Binding Energy and Mass Defect

The so-called mass defect describes the fact that the mass of an atomic nucleus with its components bound, is always smaller than the sum of the masses of its separate nucleons would be. According to Einstein's equation eq.(??) the mass can be directly converted into energy. The mass defect multiplied with c_0^2 results in the so-called binding energy. That is the energy which is needed to disassemble an atomic core into its components. Thus, in reverse, the binding energy is also the energy which is released when the separate components of a core are united. [?, p.33f] [?, p.19f] [?, p.13]

The binding energy is determined empirically through the masses of the basic components. To calculate the binding energy for any nuclide with the atomic number Z and neutron number N , the following equation can be used:

$$E_B(Z, N) = [Zm_H + Nm_n - m(Z, N)] \cdot c_0^2 \quad (1.6)$$

where m_H is the atomic mass of a hydrogen atom, m_n is the neutron mass, $m(Z, N)$ is the atomic mass of the respective nuclide and c_0 is the vacuum speed of light. [?, p.33]

An interesting value to characterise an atomic core by, is the binding energy per nucleon. Essentially, it describes how tightly the nucleons are bound within the core. Figure ?? displays the binding energy per nucleon as a function of the mass number. It can be seen that there is a maximum in the region of mass number $A \sim 60$ which means that these are the most stable nuclei. Those include for example iron, nickel and copper. But also ^4He , ^{12}C , and ^{16}O have particularly high binding energies for the region of light nuclei, which is due to the fact that each of these nuclei has the same number of 'paired' protons and neutrons. [?, p.34] [?, p.20]

For nuclei with $A > 15$, the shape of the curve shown in figure ?? can be described semi-

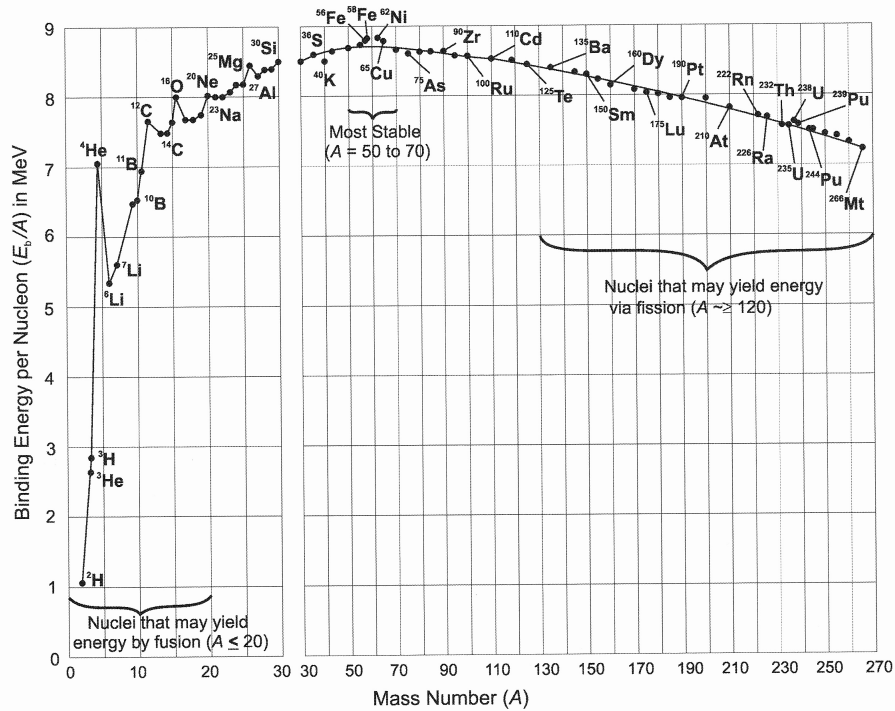


Figure 1.1: Binding energy per nucleon as a function of mass number A [?, p.20]. The most stable nuclides have mass numbers around $A \sim 60$. Nuclei with high mass numbers can be used to produce energy via fission, nuclei with low mass numbers via fusion.

empirically by the 'liquid-drop model' of the nucleus by Bethe and Weizsäcker. In this model the nucleus is compared to a drop of an incompressible liquid. The equation is the following:

$$E_B(Z, N) = [a_1A - a_2A^{2/3} - a_3Z^2A^{-1/3} - a_4(N - Z)^2A^{-1} + \delta(Z, N)] \quad (1.7)$$

where E_B is the binding energy in MeV of a nucleus with Z protons, N neutrons and a mass number A . a_1, a_2, a_3 and a_4 are coefficients with fixed values that describe the volume energy, the surface energy, the Coulomb energy and the symmetry energy. $\delta(Z, N)$ is the pairing energy term which depends on whether A, N and Z are even or odd numbers. [?, p.13] [?, p.23ff]

The shape of the curve shown in figure ?? has important consequences, especially for energy production. It signifies that energy can be yielded either by fusion of light nuclei in the range of $A < 20$ or by fission of heavy nuclei with $A \geq 120$. [?, p.33] [?, p.20]

2 Radioactive Decay and Radiation Physics

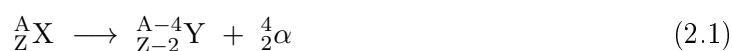
Radioactivity is a spontaneous decay process which transforms an unstable nucleus into another possibly but not necessarily stable nucleus by emitting energy in the form of radiation. The emitted radiation can either be of a particulate kind, as for instance alpha or beta radiation, or electromagnetic in the form of X-rays and gamma rays. The starting point of a radioactive transformation is called parent nucleus, the produced nuclei are called daughters. [?, p.2]

2.1 Types of Radioactive Decay

Radioactive nuclides decay spontaneously via different processes. It is important to note, that radioactive decay is largely independent of the physical and chemical state of a nuclide. It is a nuclear process that depends on the neutron to proton ratio in the core, and on the mass-energy relationship of parent, daughter and other emitted particles. Of course the various conservation laws must hold also in a nuclear reaction. The most important are the conservation of energy, linear and angular momentum and charge. [?, p.11] [?, p.19f]
The most common decay modes will now be discussed in more detail.

2.1.1 Alpha Decay

In the so-called α -decay the parent nucleus emits an α -particle, which is a ${}^4_2\text{He}$ nucleus and thus consists of two protons and two neutrons. This transformation can be written as:



In comparison to the parent nucleus, X , the daughter, Y , has a mass number which is reduced by 4 and a proton number reduced by 2. The emission of an α -particle rather than a single nucleon can be energetically more advantageous for a heavy nucleus, i.e. one with a high atomic number, because of the especially high binding energy of the α -particle. The α -particle can escape the potential barrier of the nucleus by quantum tunnelling. The probability for such an escape is dependent on the height of the Coulomb potential barrier

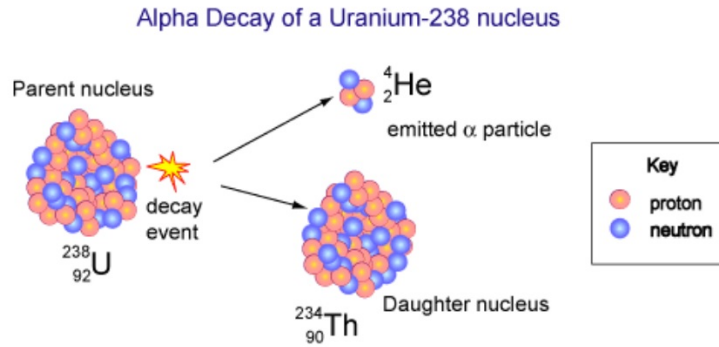


Figure 2.1: Alpha decay of ${}^{238}\text{U}$ into ${}^{234}\text{Th}$ and an α -particle [?]

as well as the energy of the particle. Decay energies of α -particles are in the area of 4 to 10 MeV. After an alpha decay most daughter nuclides remain in an excited or unstable state which leads to further decay processes. [?, p.29] [?, p.42ff]

Since an alpha particle possesses double positive charge, it is highly ionising when passing through matter. But it also has a comparatively high mass and size which corresponds to a high energy loss in matter and therefore only limited ability to penetrate matter. In air an alpha particle can only travel a few centimetres. [?, p.45ff]

As an example, figure ?? illustrates the transformation of ${}^{238}\text{U}$ into ${}^{242}\text{Th}$ via emission of an α -particle.

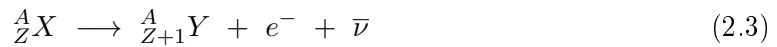
2.1.2 Beta Decay

The term beta decay, or β -decay, is used for different types of radioactive transformation processes which leave the mass number, A , unchanged but alter the number of protons. Beta decay is common if the nucleus has an excess of neutrons or protons. It is based on the ability of the nucleons to transform themselves into each other. The three most important types of beta decay are β^- -decay, β^+ -decay and electron capture. These will now be discussed in more detail. [?, p.49ff] [?, p.33ff]

β^- -**decay** is characterised by the emission of a negative beta particle, β^- , from the atomic core. When speaking of a β^- -particle, one essentially refers to an electron (also called negatron) and can therefore also write e^- instead of β^- . Principally, β^- -decay occurs in nuclei with an excess of neutrons. To stabilize the imbalance in the proton-neutron ratio, a neutron undergoes the following transformation within the nucleus:



The proton, p , remains in the nucleus, the electron, e^- , and the antineutrino, $\bar{\nu}$, are emitted. The nuclear reaction can therefore be written as:



The resulting daughter nuclide, Y , has the same mass number but the atomic number is increased by 1. [?, p.49.f] [?, p.34]

β^+ -decay, also called positron emission, occurs when a nucleus has an excess of protons and the emission of an α -particle is energetically not possible. The transformation within the atomic core takes place as follows:



A proton is transformed into a neutron, n , a positive beta particle, β^+ , which is a positively charged electron (a so-called positron, e^+) and a neutrino, ν . The neutron remains in the nucleus, the positron, e^+ , and the neutrino, ν , are both ejected.

The general equation for such a transformation is:



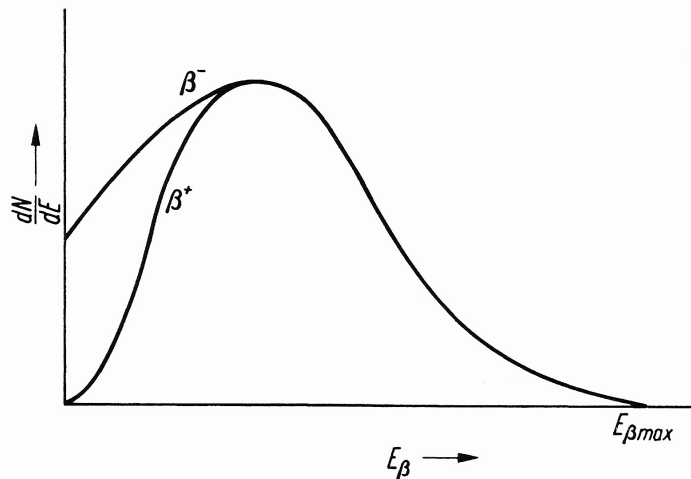
Similarly to the β^- -decay the mass number of the daughter nuclide remains the same but in this case the atomic number is decreased by 1. [?, p.34] [?, p.54f]

An ejected positron has only a short lifetime because when slowing down, it can annihilate with an electron. Their combined energy of $2m_e c_0^2 = 1.022$ MeV is released via the production of two photons with 511 keV each. The conservation of momentum dictates that these two photons are emitted in opposite directions. Thus, the gamma spectrum of a source with positron decay will always have a peak at 511 keV, which is the so-called annihilation peak. [?, p.54f] [?, p.38f]

energy spectrum for a β - decay:

Beta particles do not have discrete energies like alpha particles but display a continuous energy spectrum between zero and a specific maximum energy, E_{max} . This is due to the fact that usually only the β -particle (electron or positron) is detected but the decay energy is actually shared between the β -particle and the (anti-)neutrino. The maximum energy in the energy spectrum ranges from a few keV to MeV. Figure ?? illustrates the typical energy spectrum of a beta decay. [?, p.50ff] [?, p.81] [?, p.35]

Electron Capture (EC) is also a type of beta decay, although it does not result in the emission of a β -particle. Electron capture is an alternative competing process to β^+ -decay for nuclei with an excess of protons. Especially for heavy nuclei EC is more common than β^+ -

Figure 2.2: General energy spectrum of a β^- - and β^+ -decay [?, p.35]

decay, since the inner electron shells move closer to the core with increasing proton number. As the name already indicates, the unstable nucleus captures an electron from the atomic orbitals, most likely one of the inner K-shell, although also one of the L-shell is possible. Within the core a proton, p , combines with the captured electron, e^- , and yields a neutron, n , and a neutrino, ν . This transformation can be written as:



The neutron remains within the nucleus and helps stabilize the nucleon imbalance. The neutrino is ejected, accompanied by the emission of electromagnetic radiation in the form of internal bremsstrahlung which is due to the acceleration of the electron towards the nucleus. Generally, the process of electron capture can be described as:



In analogy with the β^+ -decay, the mass number stays the same and the atomic number is decreased by 1. [?, p.57f]

The capture of an electron by the nucleus creates a hole in the electron shell. This vacancy is filled by an electron from the outer shells which emits characteristic X-rays in this process. Instead of emitting X-rays the excessive energy can also be transferred to an electron in an outer orbital which is then emitted as a so-called Auger electron. Only these subsequent effects make the detection of electron capture possible. [?, p.57f] [?, p.38f]

Since beta particles are much lighter and have lower charge, they are not as ionising as alpha particles when passing through matter. But these same properties allow a beta particle to penetrate much further into matter than an alpha particle with equivalent energy could. The

absorption of beta particles in matter displays an exponential character which is dependent on the material itself and its thickness. [?, p.65ff]

2.1.3 Internal Conversion

Internal conversion is a type of decay which is characterised by the emission of an atomic electron. An unstable excited nucleus can reach a stable state by transferring its excessive energy to an atomic electron which is thereafter ejected as a so-called internal conversion electron. This process is in fact a competing process to gamma ray emission and they often occur simultaneously in the same radionuclides. The kinetic energy of the electron is the nuclear de-excitation energy minus its atomic binding energy. Thus, the electrons which originate from internal conversion show discrete energy lines, unlike the ones from beta decay which are characterised by a broad energy spectrum. [?, p.68f]

2.1.4 Neutron or Proton Emission

Although it is not very common amongst radionuclides, it is also possible that a single nucleon, proton or neutron, is ejected from the core. [?, p.48ff]

Proton emission happens mostly directly after emission of a positron. This transformation can be written as:



The emission of a neutron can occur directly after a β^- -decay of fission products whenever the energy is higher than the binding energy of a neutron. The equation for neutron emission is:



2.1.5 Spontaneous Fission (SF) and Neutron-Induced Fission

Nuclides with a high mass number can decay via spontaneous fission rather than alpha decay. Spontaneous fission describes a process where the nucleus –spontaneously and without inducement– splits into two fission fragments plus several neutrons. The fission fragments can of course decay further, via other decay modes. Because of the additional neutrons, the process of spontaneous fission can be used for the production of neutrons. For instance ${}^{252}\text{Cf}$ is a commonly used laboratory neutron source. [?, p.77f]

Another form of fission is neutron-induced fission. A popular example for this process is the transformation of ${}^{235}\text{U}$, since it is used in nuclear fission reactors. When a nuclide of ${}^{235}\text{U}$ is

exposed to slow, so-called thermal, neutrons, it can capture a neutron and form ^{236}U . This event is followed by two scenarios: In around 14% of the cases the unstable ^{236}U decays via emission of an α -particle and gamma rays with a half-life of $2.4 \cdot 10^7$ a to ^{232}Th . Nevertheless, the more probable scenario is that the ^{236}U nucleus becomes an unstable oscillating droplet which finally splits into two fragments releasing around 194 MeV of energy. This energy is mostly in form of kinetic energy of the fission fragments. In addition to the fission fragments which generally do not have to be of the same size, also a number of neutrons is released. That is called the yield of neutrons which is averagely around 2.42. These additional neutrons are highly important for sustaining a chain reaction in a nuclear fission reactor which will be discussed in more detail in chapter ?? [?, p.78f]

Below, there is an example of one of the many possible fission reactions to illustrate neutron-induced fission of ^{235}U :



The fission products in this example are strontium and xenon, accompanied by the release of 3 neutrons. Strontium and xenon are both unstable and decay via various decay modes until they reach a stable ground state. The energy which is released in this particular reaction, including the decay of the fission fragments until they are stable and the released neutrons which have an average energy of 2 MeV each, is around 200 MeV. [?, p.78f] [?, p.103f]

2.1.6 Electromagnetic Radiation

In the course of a radioactive transformation also high-energy electromagnetic radiation can be emitted, which is why it is important to recall the dual nature of electromagnetic radiation: It can exhibit properties of a wave as well as a particle, a so-called photon. The energy of a photon is given by the Planck-Einstein relation:

$$E = h\nu = \frac{hc}{\lambda} \quad (2.11)$$

where h is the universal Planck constant ($h = 6.626 \cdot 10^{-34}$ Js), ν the photon frequency, λ the wavelength and c the vacuum speed of light ($c = 2.9979 \cdot 10^8$ m/s). [?, p.90f]

The most common forms of electromagnetic radiation for radionuclide decay processes are gamma rays and X-rays. Those two will be discussed below.

Gamma Emission and Isomeric Transition

Most nuclei remain in an excited energy state after a decay process. Such nuclides are called isomers and the process, which describes the transition from higher to lower energy or the ground state, is called isomeric transition. The gamma rays that are emitted have discrete energies, precisely the difference between the two energy levels. That can be written as:

$$E_\gamma = h\nu = E_1 - E_2 \quad (2.12)$$

where E_γ is the energy of the photon, h is Planck's constant ($h = 6.626 \cdot 10^{-34}$ Js), ν the photon frequency and E_1 and E_2 refer to the higher and lower energy level respectively. The energy of gamma rays ranges from a few hundred keV to a few MeV. [?, p.92] [?, p.39f]

The radioactive transformation by gamma ray emission can be written as:



Noticeably, neither the mass number nor the proton number changes in this process. The superscript star (*) indicates the excited state of the nuclide. [?, p.40]

Usually isomeric transition happens almost immediately after the previous decay process, but sometimes the de-excitation is hindered because of a so-called forbidden transition. This can occur if there is a large spin difference between the energy levels. Then the lifetime can range from seconds to years and one talks of the nuclide being in a metastable state. Such metastable nuclides are denoted by a 'm' next to their mass number, for instance ${}^{60\text{m}}\text{Co}$. [?, p.14]

X-rays

X-rays are another form of electromagnetic radiation and similar to gamma radiation. But whereas gamma ray emission originates from the de-excitation of an excited nucleus, X-rays stem from electron energy transitions. X-rays are divided into two types which are distinguished by their energy spectrum. Transitions of electrons in the atomic shell create X-rays with discrete energy lines. Electrons or other charged particles that are accelerated towards the nucleus are deflected by the Coulomb field and create a broad continuous energy spectrum. This form of radiation is also called 'bremsstrahlung'. [?, p.94ff]

2.2 Activity and Decay Law

Radioactive transformation is a statistical process. Every nucleus of the same type of radionuclide has the same probability of decay. The probability that a particular nucleus decays in a certain time period is independent of its history. That means two nuclei of the same radionuclide have the same probability of transformation within a certain time period, even if they have been formed at different times. [?, p.19ff] [?, p.19]

The activity of a radioactive sample is proportional to the number of radionuclides in the sample. Per definition, it is the mean number of decay processes per unit time. This may be expressed as:

$$A = -\frac{dN}{dt} \quad (2.14)$$

where A is the activity and dN is the number of nuclides which disintegrate in a time period, dt . The SI unit for activity is becquerel (Bq). One becquerel corresponds to one disintegration per second. Another outdated unit for activity is curie (Ci) which was defined by the activity of 1 g pure ^{226}Ra . Since this is a very large unit it was commonly replaced by the unit of becquerel. The transformation between those two units of activity is:

$$1 \text{ Ci} = 3,7 \cdot 10^{10} \text{ Bq. [?, p.22f] [?, p.7]}$$

It is important to note that the activity depends on the amount of radioactive material and is an extrinsic quantity. As a consequence of radioactive decay, the activity decreases over time, the rate of which is given by the so-called half-life. It denotes the time period which is needed to halve the activity of a radionuclide sample. [?, p.135] [?, p.23]

If there is a particular number of radionuclides, N , at a given time, t , in a homogeneous sample then a certain amount of nuclides, dN , will disintegrate within a time period, dt . This can be written as:

$$dN = -\lambda N dt \quad (2.15)$$

where λ is a decay constant which is a measure for the probability of decay.

Integrating this equation from the starting time ($t_0=0$) to the time t and between the limits of N_0 , which is the initial number of nuclides, and N , which is the number of nuclides after the time period, t , has passed

$$\int_{N_0}^N \frac{dN}{N} = -\lambda \int_{t_0=0}^t dt \quad (2.16)$$

gives the following equation:

$$\ln N(t) - \ln N_0 = -\lambda t \quad (2.17)$$

This leads to the so-called decay law, which describes the decay of a radionuclide sample: "[...] the ratio of the number of radionuclides, N , in a sample at a given time, t , to the original number of nuclides, N_0 , in that sample at time $t=0$, is equal to $e^{-\lambda t}$ where e is the

base to the natural logarithm, λ is a decay constant of that radionuclide and t is the interval of time.” [?, p.136]. This may be written as:

$$N = N_0 \cdot e^{-\lambda t} \quad (2.18)$$

In terms of activity, A , this can also be expressed as:

$$A = A_0 \cdot e^{-\lambda t} \quad (2.19)$$

where A is the activity at a given time, t , and A_0 is the original activity at $t=0$. [?, p.20ff] [?, p.136ff]

The inverse of the decay constant, λ , is called the mean lifetime τ :

$$\tau = 1/\lambda \quad (2.20)$$

This mean lifetime represents the time period until the activity of a sample has decreased to $1/e$ of its initial value.

Another very important constant which was briefly mentioned above, is the so-called half-life $T_{1/2}$. The half-life is the time period after which the activity is one half of its original value, meaning also the number of nuclei has decreased to half the initial value. After one half-life there is only half of a number of nuclides left, after two half-lives it is one quarter, etc. [?, p.21] [?, p.7f]

Through eq. ?? a connection between $T_{1/2}$ and λ can be obtained:

$$T_{1/2} = \frac{\ln 2}{\lambda} = \tau \ln 2 \quad (2.21)$$

In figure ?? the decay law with its exponential behaviour is illustrated by means of a linear and semi-logarithmic plot. It can be seen clearly in both illustrations that after one half-life only half of the initial number of nuclides is left.

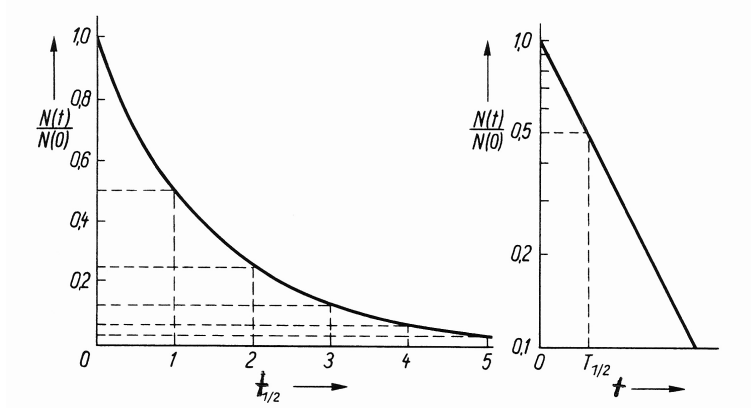


Figure 2.3: Illustration of the decay law with a linear (left) and semi-logarithmic (right) scale [?, p.21]

2.3 Decay Chains

In nuclear decay it is very common that the daughter products are also radioactive. In such a case one speaks of a decay chain. [?, p.23f]

Considering a decay process with a parent nuclide A and a daughter nuclide B, three cases can be distinguished, depending on the half-lives of the parent and daughter:

- If $T_{1/2A} \gg T_{1/2B}$ ($\lambda_A \ll \lambda_B$) the parent half-life is much longer than the half-life of the daughter nuclide, and one talks of a secular equilibrium.
- If $T_{1/2A} \geq T_{1/2B}$ ($\lambda_A < \lambda_B$) the half-life of the parent is longer than the one of the daughter but not as much as in the case of a secular equilibrium. This condition is called transient equilibrium.
- If $T_{1/2A} < T_{1/2B}$ the half-life of the parent is shorter than the half-life of the daughter and therefore no equilibrium can be achieved.

Decay chains make the calculation of activities for daughter nuclides more complicated, but they are an important aspect to consider, when trying to detect a certain decay which overlaps with others. [?, p.24ff] [?, p.141ff]

2.4 Interaction of Electromagnetic Radiation with Matter

This section is an attempt to give a quick overview over the possible mechanisms of interaction of electromagnetic radiation with matter. Since electromagnetic γ - and X-rays do not have charge or rest mass, they can penetrate deeper into matter than alpha or beta particles. In the end they are absorbed nonetheless. [?, p.105]

2.4.1 Photoelectric Effect

An atom may absorb the entire energy of a photon and transfer this energy to an electron which is subsequently ejected. The energy of the released electron is:

$$E(e^-) = h\nu - E_B(e^-) \quad (2.22)$$

where $E(e^-)$ is the energy of the emitted electron, $h\nu$ is the photon energy and $E_B(e^-)$ denotes the binding energy of the electron. The emitted electron is practically a β -particle and has ionising effects when passing through matter. [?, p.105]

2.4.2 Compton Effect

The Compton effect, also known as Compton scattering, is another mechanism in which the energy of a photon is transferred to an atomic electron. But in contrast to the photoelectric effect, here only part of the photon energy is imparted to the electron. The photon is deflected with a reduced energy at a certain angle and the electron is ejected likewise at another angle. Both particles travel further through matter, the photon until its energy is fully dissipated by interaction with other electrons and the electron is again identical to a β -particle and loses its energy through ionisation. [?, p.105ff]

The energy of the ejected electron, the so-called Compton electron, is:

$$E(e^-) = E_\gamma - E'_\gamma - E_B(e^-) \quad (2.23)$$

where $E(e^-)$ is the energy of the emitted electron, E_γ and E'_γ are the photon energy before and after collision with the electron respectively and $E_B(e^-)$ is the binding energy of the electron. [?, p.107]

The interactions of Compton electrons and scattered photons with matter result in the typical Compton edge and backscatter peak in gamma spectra.

2.4.3 Pair Production

Pair production describes the effect that from the photon energy matter is created. A photon that interacts with the Coulomb potential of the nucleus, is converted into an electron, e^- , and a positron, e^+ . For pair production to take place, the photon has to have at least the energy equivalent to the masses of the two particles. This can be written as:

$$E_{pair} = m_{e^-}c_0^2 + m_{e^+}c_0^2 = 2mc_0^2 = 2 \cdot (0.511 \text{ MeV}) = 1.022 \text{ MeV} \quad (2.24)$$

where E_{pair} is the energy needed for pair production and m_{e^+} and m_{e^-} are the masses of the positron and electron respectively. The excess photon energy appears as kinetic energy of the two particles. [?, p.107f]

Pair production can not only occur when a nucleus is exposed to gamma radiation but also as a competing process to gamma ray emission itself. When the gamma transition energy is higher than 1.022 MeV this internal pair production is possible. [?, p.108]

2.4.4 Attenuation

To reduce the intensity of γ - or X-rays, absorbing materials with high densities and large atomic numbers are being used. The radiation intensity decreases exponentially with thickness of the absorbing material, x . Expressed as an equation this is:

$$I = I_0 e^{-\mu x} \quad (2.25)$$

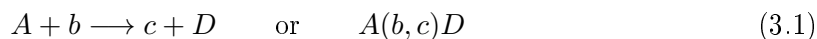
where I_0 and I are the initial and 'after-absorption' gamma ray intensities, x is the thickness of the absorber and μ is the so-called linear attenuation coefficient.

The linear attenuation coefficient depends on the material. In fact, it consists of the attenuation coefficients of the independent photoelectric, Compton and pair production processes. [?, p.111f]

3 Nuclear Reactions

3.1 Reaction Types

In a nuclear reaction two nuclear particles interact to form a new product nucleus or particle. A general reaction can be written in the following form:



where A is the target nucleus, b the incident particle, the so-called projectile, D the product or residual nucleus and c the ejected particle. The most important types of reactions are briefly covered below. [?, p.37ff] [?, p.56ff]

Elastic scattering: The particles collide but the target nucleus is not changed and the particle that is ejected is the same or of the same sort as the incident particle.

Inelastic collision: The particles collide and the nucleus is excited into a higher energy level. The incident and ejected particle are of the same sort but the one ejected has lower kinetic energy due to the excitation of the target nucleus.

Exchange reaction/compound nuclear reaction: This is the classical reaction described by eq. ???. The projectile, b , hits the target nucleus, A , a new nucleus, D , is formed and another particle, c , is ejected. Not always but in most cases, this reaction takes place in two steps: First, the formation of a compound nucleus from the projectile and target. And thereafter, the decay of this compound nucleus, which has an immeasurably short mean lifetime, into the product nucleus and the ejected particle. Typical reactions of this sort are (n,p), (n, α), (p,n), (p, α), (d,n), (d,p), (α ,n), and (α ,p) reactions.

Pickup and stripping reactions: High-energy projectiles do not have to interact with all of the nucleons in the target but only with a few. The projectile can pick up some of the nucleons or it can lose some of its own nucleons to the target core.

Spallation reactions: Nuclear spallation occurs if the projectile is a charged particle with high energy (>100 MeV). The target nucleus loses some nucleons instantly in the collision. The residual nucleus often remains in an excited state and decays into several smaller components. Since many neutrons are emitted in such a reaction, the spallation reaction is

generally considered a good neutron source.

Nuclear fission: When a high-energy charged particle strikes a heavy nucleus, such as ^{235}U , the target nucleus is split into two fragments and additionally two or three neutrons are released. Nuclear fission and neutron-induced fission are discussed in more detail in section ??.

3.2 Q-value of a Reaction

Energy calculations of nuclear reactions are based on the mass difference of the participating nuclear particles. The so-called Q-value describes this energy of a reaction. If the Q-value of a reaction is positive, energy is released during the reaction which is then called exothermic. If the Q-value is negative, energy is required for the reaction to take place and it is called endothermic. The Q-value can be written as:

$$Q = E_{\text{React}} - E_{\text{Prod}} = (m_{\text{React}} - m_{\text{Prod}})c_0^2 \quad (3.2)$$

where the index 'React' denotes the energy or rest mass of the reactants of a reaction and the index 'Prod' describes the products of a reaction respectively. [?, p.39f]

3.3 Reaction Cross Section

The reaction cross section describes the probability that a particular nuclear reaction will take place. It is not the true cross section of a nucleus, rather the effective area. The larger the reaction cross section of a target nucleus, the higher the probability for an interaction with the projectile particle.

The reaction cross section has the dimension of an area and is given in m^2 or cm^2 . Previously, the outdated term of barn (b) was used and can still be found in many texts ($1 \text{ b} = 10^{-24} \text{ cm}^2$). It is important to note, that the reaction cross section is only a descriptive measure for the probability of an interaction and has nothing to do with the actual dimension of the atomic core. The geometric cross section of a nucleus is in the area of 10^{-24} cm^2 whereas the reaction cross section for neutron capture can be 10^{-19} cm^2 for some nuclides. [?, p.41]

The probability of a nuclear reaction to take place depends on the rate at which the projectiles are hitting the target material. This rate of a nuclear reaction, R , measured in number of ejected particles per second, is dependent on the intensity of the projectile beam, I , the density of the target nuclei in the target material, n , the reaction cross section, σ , and the

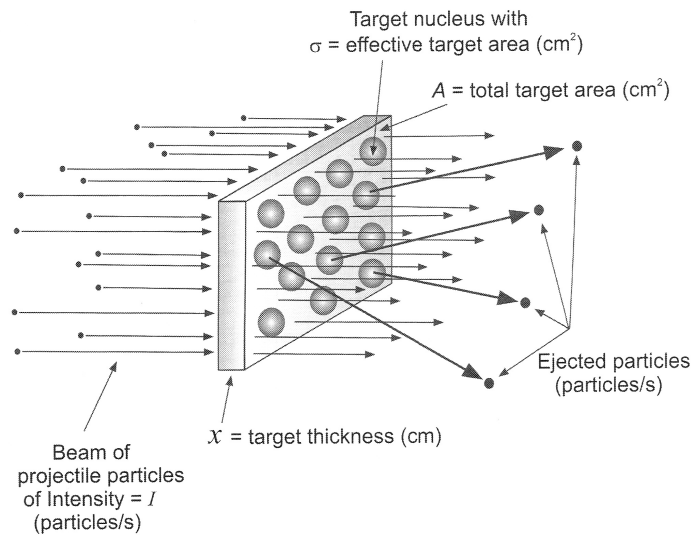


Figure 3.1: Illustration of the reaction target area [?, p.41]. A target consisting of nuclei with cross section σ with area A , and thickness x , is bombarded by a beam of particles. Some of these projectiles interact with the target nuclei, producing other particles which are ejected subsequently.

thickness of the target material, x . This can be written in form of an equation as:

$$R = In\sigma x \quad (3.3)$$

Figure ?? displays the reaction target area, where a projectile beam hits a target material containing nuclei with a reaction cross section σ . Some projectile particles interact with the target nuclei, resulting in the emission of product particles. These ejected particles can be detected and in this way the reaction rate can be calculated. [?, p.41]

3.3.1 Partial and Total Cross Section

In general, not only one reaction is possible but a multitude. Every possible reaction has its own partial cross section, meaning the possibility that this particular reaction takes place. The total cross section is the sum of all the partial cross sections. Primarily, one can distinguish between scattering and absorption reactions, which are described by σ_s and σ_a respectively. These two can be further divided, for example into elastic and inelastic scattering and absorption with subsequent fission, etc. [?, p.19] [?, p.21f] [?, p.12f]

The total cross section can therefore be written as:

$$\sigma_{tot} = \sigma_s + \sigma_a = \sigma_e + \sigma_i + \sigma_f + \dots \quad (3.4)$$

3 Nuclear Reactions

The reaction cross section is in fact energy dependent. When plotted over time, three regions can be distinguished: the low energy part where the cross section is inversely proportional to the neutron energy, the medium-energy area or so-called resonance area where high resonances with very high cross sections can occur and the high-energy region where the resonance peaks grow wider. As an example, the reaction cross section for the (n,γ) reaction of ^{197}Au plotted over the neutron energy can be seen in figure ?? [?, p.21f]

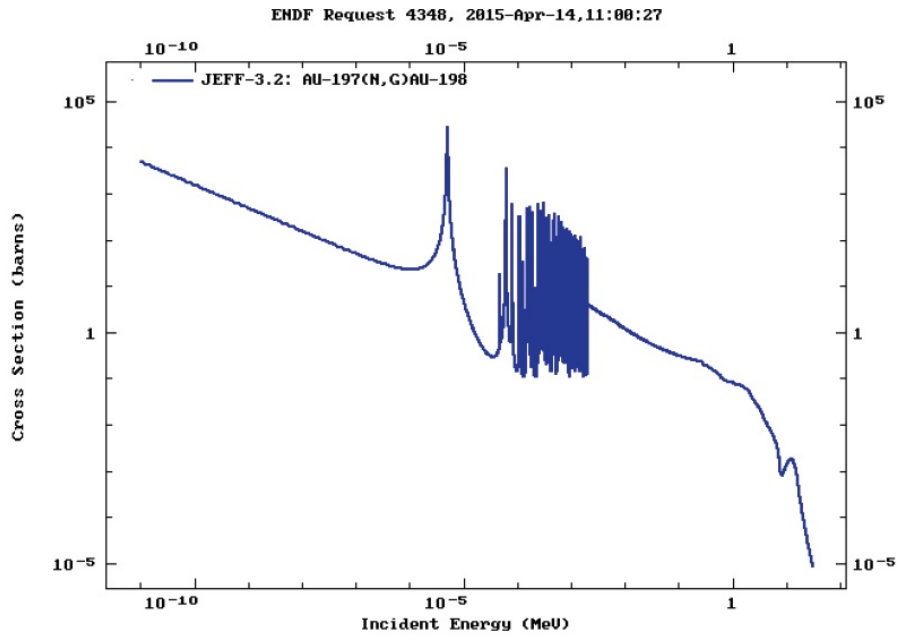


Figure 3.2: The reaction cross section for the (n,γ) reaction of ^{197}Au as a function of incident neutron energy. [?]

4 A Nuclear Reactor as a Neutron Source

Generally speaking, a nuclear reactor is a facility for initiation, maintaining and control of a fission chain reaction. A reactor consists of the reactor core with the nuclear fuel, a moderator, a reflector, a control system and shielding. Nuclear reactors are the most powerful neutron sources reaching neutron flux densities of up to $10^{15} \text{ cm}^{-2}\text{s}^{-1}$ which makes them the most important irradiation facility for neutron activation analysis as well as for many other applications. [?, p.26]

4.1 The Configuration of a Nuclear Fission Reactor

Inside the reactor core there are the fuel elements which are enriched with a fissionable element, most commonly ^{235}U . Upon the fission of a ^{235}U nucleus an average of 2.42 neutrons with a medium energy of 2 MeV are produced. To induce further fission processes these fast fission neutrons, or so-called prompt neutrons, have to be slowed down to lower energies. This deceleration takes place by means of a moderator. Materials with good moderating properties have to have a large braking capacity and a low tendency to absorb neutrons, meaning a small neutron absorption cross section. The most widely used moderator materials are light water (H_2O), heavy water (D_2O), graphite and beryllium. [?, p.14] [?, p.27]

The fission chain reaction is controlled and regulated by absorber or regulating rods. These rods are made of materials with high neutron absorption cross sections, for instance cadmium or boron compounds. The total insertion of these absorber rods into the core is followed by a heavy decrease in the neutron flux and the stop of the fission for lack of neutrons to maintain the chain reaction during operation. [?, p.14] [?, p.27]

The reactor core is surrounded by a so-called reflector which is also made of a moderating material. The purpose of the reflector is to reduce the loss of neutrons. The minimization of radiation exposure outside of the reactor is ensured by the shielding which is made of graphite, water or heavy concrete. A cooling system discharges the energy released during the fission process which can be used for the production of (electrical) energy, as is done in nuclear power plants. [?, p.14] [?, p.27]

Nuclear reactors can be distinguished by various features. First of all, the intended purpose, which can be research, performance, or breeding. Another good distinction is the fuel material and its enrichment, for example ^{235}U , ^{239}Pu , ^{233}U , and also the moderating and cooling material. [?, p.14] [?, p.28]

4.2 Reactor Neutron Energy Spectrum

In the fission process of ^{235}U the produced neutrons have a wide energy range from below 0.1 MeV to up to 20 MeV. By means of a moderator these high-energy neutrons are slowed down to lower energy regions. Plotting the number of neutrons over their energy, results in the so-called neutron energy spectrum. A typical reactor neutron spectrum can be seen in figure ???. This is only a qualitative illustration, which will be slightly modified in any particular case due to effects like moderation and neutron escape etc. [?, p.15f]

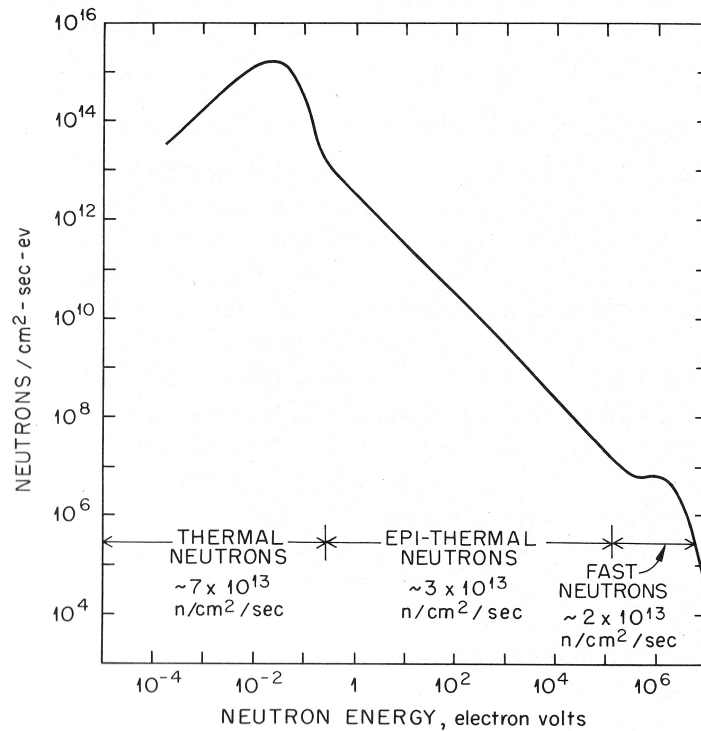


Figure 4.1: A typical reactor neutron energy spectrum [?, p.15]. Neutrons can be distinguished according to their energies into thermal, epithermal and fast neutrons.

As can be seen in figure ??, the neutron spectrum is divided into three regions with regard to the neutron energy: the region of thermal neutrons with energies below 0.2 eV, the epithermal neutrons with energies between 0.2 eV and 0.1 MeV and the region of fast neutrons with energies above 0.1 MeV. When a neutron has been slowed down to thermal energies, i.e.

energies below 0.2 eV, it is referred to as a 'thermal neutron'. The most probable velocity of a thermal neutron at 20°C is 2200 m/s. It is important to note, that the exact definition of the neutron energy regions can vary and should not be taken as fixed. [?, p.14f]

The reactor neutron population at a certain constant power is usually steady over time, in particular over a few hours. But with the geometric structure of a reactor in mind, it becomes apparent, that the shape of the neutron spectrum is highly dependent on the exact position in the reactor. Close to fuel elements the reactor spectrum looks similar to a fission neutron spectrum. With increasing distance from the fuel or the core the spectrum changes. That effect can be attributed to moderation, geometry effects, used materials etc. [?, p.16]

5 Radiation Detection

5.1 Basic Principle

The detection of radiation is based on the basic principle of transferring all or part of the radiation energy to the detector and converting it to some other form of energy, like for instance an electrical impulse which is then treated further with electronic means. Practically all modern detectors use the conversion into electrical impulses because due to the development on the electronics and computer sector this is a very accurate and fast way to treat information. How the radiation energy is converted, depends on the detector type. Some detectors collect the electrons produced by the ionising radiation, while others use the ionising effect indirectly through the collection of emitted light or a chemical reaction. Whatever method of detecting radiation is used, there are a few fundamental terms which are important for radiation detectors in general. Those will be discussed below. [?, p.107]

5.2 General Terms

One of the most important characteristics is the detector sensitivity. A detector is usually designed to be sensitive to a certain type of radiation within a defined energy region. For any other type of radiation or outside the energy range the detector will most likely be useless. [?, p.107f]

In case the energy of the radiation is of interest, it is important that the output signal can be put into direct relation with the radiation energy. This property is referred to as the detector response. The response is dependent on the energy range and on the type of particle which should be detected. The most significant factor when measuring radiation energy is the energy resolution. That means how well the detector can distinguish two energies which lie very close to each other. [?, p.108ff]

Also the response time, which is the time it takes, to produce a signal after the radiation has arrived in the detector mass, is of great importance. The signal should be formed quickly and it should not be long itself because that could lead to a piling up of signals. This piling up is considered in another important characteristic of a detector: the dead time. The dead

time is the time it takes to process a signal. When the duration of a signal is long and the detector keeps sending signals the events will pile up. The signal will be distorted and information will get lost. It can also happen that the detector is insensitive while a signal is being processed which of course results in the loss of any other event which arrives during that time. [?, p.112]

Last but not least the detector efficiency is a crucial characteristic. The total or absolute efficiency refers to the in the detector registered events compared to all the events which are emitted by the source. When talking about the total efficiency one has to consider the geometry of the detector, which is described by the geometric efficiency, and intrinsic effects. Those are defined by the intrinsic efficiency, meaning the registered events compared to the events which are actually hitting the detector. [?, p.113]

6 Counting Statistics

A measurement process will always contain uncertainties. In the case of a radioactive sample it is even more complicated, because radioactive decay is a random process itself. For that reason, this section is about counting statistics and statistical distributions. [?, p.163]

6.1 The Binominal Distribution

The binominal distribution is a discrete probability distribution. Considering a single experiment, p is the probability of success and $1 - p$ is the probability for failure, meaning that the expected event did not take place. When this same experiment is repeated independently n times, the probability for having x successes, $P(x)$, is given by the binomial distribution:

$$P(x) = \frac{n!}{(n-x)!x!} \cdot p^x \cdot (1-p)^{n-x} \quad (6.1)$$

where x and n are integer values, with $x=0,1,2,\dots,n$. The summation of all possible probabilities $P(x)$ is one. This is called the normalization condition and can be written as:

$$\sum_{x=0}^n P(x) = 1 \quad (6.2)$$

The mean value of a binomial distribution is given by:

$$\bar{x} = \sum_{x=0}^n xP(x) = np \quad (6.3)$$

The variance σ^2 and standard deviation σ are:

$$\sigma^2 = \bar{x}(1-p) \quad (6.4)$$

$$\sigma = \sqrt{\bar{x}(1-p)} \quad (6.5)$$

The standard deviation describes the fluctuation in a distribution, and is sometimes used as a means to describe uncertainty.

In case of a radioactive decay, n can be interpreted as the number of radionuclides in the sample, x as the number of radioactive transformations in a time period t and p as the

probability that a nucleus decays in that time period t ($p = 1 - e^{-\lambda t}$). [?, p.26f]

6.2 The Poisson Distribution

In case of a small but constant probability of success, p , and a large number of experiments, n ($n \gg x$), a random process is described by the Poisson distribution instead of the binominal distribution. The Poisson distribution is used not only for radioactive decay but describes many other (daily life) processes, like for instance the number of misprints on a book page.

To describe radioactive decay by means of the Poisson distribution, the total number of radionuclides in a sample should be large and the probability of decay should be constant for each nuclide and independent of the other nuclides. Also, the half-life should be long in comparison to the detection pulse.

The Poisson distribution can then be written in the form of:

$$P(x) = \frac{pn^x e^{-pn}}{x!} = \frac{\bar{x}^x e^{-\bar{x}}}{x!} \quad (6.6)$$

where $P(x)$ describes the probability that a number of x decays takes place during a certain time period, t . As can be seen in the simplification, with the help of the mean value, \bar{x} , there is no need to know the specific probability of success, p , or the exact number of experiments, n . [?, p.27] [?, p.164f] The normalization condition for the Poisson distribution is:

$$\sum_{x=0}^{\infty} P(x) = 1 \quad (6.7)$$

The variance and standard deviation of the Poisson distribution are given by:

$$\sigma^2 = \bar{x} \quad \text{and} \quad \sigma = \sqrt{\bar{x}} \quad (6.8)$$

6.3 The Gaussian Distribution

If not only the number of experiments, n , is large but also the mean value, \bar{x} , the Poisson distribution can be transformed into the Gaussian distribution, which is given by:

$$P(x) = \frac{1}{\sqrt{2\pi\bar{x}}} \cdot e^{-\frac{(x-\bar{x})^2}{2\bar{x}}} \quad (6.9)$$

The variance and standard deviation are the same as for the Poisson distribution. [?, p.28] [?, p.165f]

7 Radiation Protection and Dose Rates

The International Commission on Radiological Protection gives recommendations, which aim to protect human health and the environment against the harmful effects of radiation exposure.

7.1 The Principles of Radiological Protection

Radiological protection is based on the following three general principles. These principles are relevant for emergency situations as well as for planned exposure situations, which include occupational, public and medical exposure. The first two principles are source-related, which means that they apply in all situations of exposure. The third principle relates to an individual and applies in exposure situations which are planned. [?]

- The principle of justification says that "any decision that alters the radiation exposure situation should do more good than harm". [?, p.88]
- The principle of optimisation of protection says that "the likelihood of incurring exposures, the number of people exposed, and the magnitude of their individual doses should all be kept as low as reasonably achievable, taking into account economic and societal factors". [?, p.89] This is also known as the ALARA principle due to the phrase "as low as reasonably achievable".
- The principle of application of dose limits says that "the total dose to any individual from regulated sources in planned exposure situations other than medical exposure of patients should not exceed the appropriate limits recommended by the Commission". [?, p.89]

7.2 Biological Effects

There are two general categories which characterise the detrimental health effects of radiation exposure [?]:

- Deterministic effects are harmful tissue reactions which are mostly of an acute nature and follow the exposure of high doses. They are mostly a result of the killing or malfunction of cells. These effects only appear if a certain threshold value of dose is exceeded.
- Stochastic effects (cancer and heritable effects) arise from high as well as low doses and can be observed through the increasing occurrence of these effects long after exposure. The mutation of somatic cells can cause cancer development in the exposed individual, and the mutation of reproductive cells can lead to heritable disease in the offspring of the exposed individual.

Deterministic effects are characterised by a certain threshold dose below which these harmful tissue reactions do not occur. Above the threshold dose the radiation damage increases with increasing dose. The dose threshold is dependent on the organ or tissue which is exposed. Nevertheless, up to 100 mGy absorbed dose, no tissue is damaged on a clinically relevant scale. This applies in the case of receiving a single acute dose and in the case of receiving low doses spread over a longer time period, for example repeated annual exposure. To prevent the development of deterministic effects there are dose limits for occupational and public radiation exposure which also include the equivalent dose limits for hands/feet, skin, eyes, etc. [?]

Concerning stochastic effects, their probabilistic nature makes it impossible to clearly distinct between 'safe' and 'dangerous'. Radiological protection continues to use the 'linear-non-threshold' (LNT) model. It is a dose-response model that is "based on the assumption that, at doses below about 100 mSv, a given increment in dose will produce a directly proportionate increment in the probability of incurring cancer or heritable effects attributable to radiation". [?, p.51] That means that one has to assume some risk, however small, and the protection depends on what is regarded acceptable. In spite of the fact that there is still no direct evidence that radiation exposure of parents causes heritable disease in offspring, this risk for future generations is nevertheless included in radiological protection. [?,?]

7.3 Dose Quantities

In dosimetry various different units are being used. That is due to the fact that radiation ionises or at least excites the atoms or molecules making up a material. One can distinguish between the amount of energy which is deposited in a material or the quantity of ionisation. [?]

7.3.1 Absorbed Dose

Probably the most important quantity for radiological protection is the absorbed dose D . It is defined as

$$D = \frac{d\bar{\varepsilon}}{dm} \quad (7.1)$$

where dm is a mass element and $d\bar{\varepsilon}$ is the mean energy which is imparted to matter by ionising radiation. The unit of absorbed dose is J/kg which has the distinctive name of gray (Gy). Absorbed dose is a measurable quantity which is often averaged over tissue volumes and organs for practical applications. However, the absorbed dose gives no information about the type of radiation or about the rate of the irradiation. Both of which are significant parameters for the consideration of biological effects. [?] [?, p.70]

7.3.2 Equivalent Dose

The biological damage depends strongly on how ionising a particle is. That is called the relative biological effectiveness. Therefore, specific types of radiation, and also their energies, are assigned a quality factor or radiation weighting factor for radiation R, w_R . Using this factor and the average absorbed dose, another new dose rate can be introduced. The equivalent dose H_T is supposed to give a good measure of the biological damage created by radiation in an organ or tissue. It is defined as:

$$H_T = \sum_R D_{T,R} w_R \quad (7.2)$$

where $D_{T,R}$ is the averaged absorbed dose in a specific organ or tissue T caused by radiation of the type R, and w_R is the above introduced radiation weighting factor. The equivalent dose has the SI unit of J/kg with the special name of sievert (Sv). The sievert has the same dimension as the gray but it indicates that the type of radiation has been considered and therefore also that this value was not measured but calculated. [?] [?, p.71f]

7.3.3 Effective Dose

To account for the fact that the biological effects depend on the particular organ or tissue, which is exposed to radiation, the so-called tissue weighting factor w_T is introduced. This factor does not depend of the type or energy of radiation but only on the organ or tissue (in reverse to the radiation weighting factor).

Taking this new factor into account, the effective dose E is defined as:

$$E = \sum_T w_T H_T = \sum_T w_T \sum_R w_R D_{T,R} \quad (7.3)$$

The unit of effective dose is J/kg and –in correspondence to the equivalent dose– also has the specific name of sievert (Sv). [?] [?, p.73]

Part II

Methods and Materials

8 Neutron Activation Analysis

8.1 Principle of Neutron Activation Analysis (NAA)

"The principle of activation analysis is that a particle (neutron, proton, α -particle, etc.) or photon (γ -rays, bremsstrahlung) induces a nuclear reaction in an atom of a target element. The product of the reaction is detected and quantified by prompt photon or particle emission or, more commonly, by its decay properties, if radioactive." [?, p.1930]

As the name implies, in the case of neutron activation analysis neutrons are being used as the reaction inducing particles. The method of NAA was developed in 1936 by Hevesy and Levi. Furthered by the introduction of nuclear reactors as neutron sources with high intensities in the 1940s and the development of NaI(Tl) and Ge(Li) gamma ray detectors in the 1960s, it became a widely used practical analytical method. It is used especially as a method of determination of trace elements in many fields such as biology, for example in environmental as well as health related and nutritional studies, geology and material sciences. [?, p.1930] [?, foreword]

NAA is a very sensitive and non-destructive method of analysis. Other advantages of this method include high accuracy, comparatively small interferences and matrix effects and almost non-existent blank contributions. The physical and chemical structure of the sample do not affect the activation and induced activity much and therefore the composition of the matrix of the material during and after irradiation does not matter particularly. Interferences can arise when other radionuclides with similar gamma ray energies are produced during irradiation. This can be avoided by reducing the concentration of the interfering elements or suppressing certain interfering reactions which are often fast neutron reactions. [?, p.1934f]

The biggest disadvantage of NAA is the need for a nuclear reactor as a neutron source. Other disadvantages –in comparison to other analysis methods– are the radioactivity of the sample which calls for safety procedures and radiological protection and the long time it takes to analyse some elements. [?, p.1935]

To demonstrate the principle of NAA, the activation of aluminium is taken as an example. A nuclear reaction can have many channels of decay, for Al the major channels are displayed in figure ??.

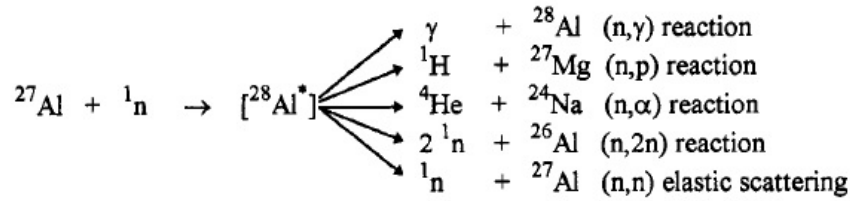


Figure 8.1: The major decay channels for ${}^{28}\text{Al}^*$ after neutron activation of ${}^{27}\text{Al}$ [?, p.1930]

${}^{28}\text{Al}^*$ denotes the compound nucleus which has a very short lifetime and decays further into the other products. The (n,n) reaction is called elastic scattering and is the only one that does not leave a radioactive product. [?, p.1930]

Thus, a neutron can induce various nuclear reactions, mainly depending on its energy. Neutrons with energies below 0.1 eV are called thermal, between 0.1 and 100 eV epithermal and above that they are called fast neutrons. The cross section for thermal and epithermal neutron reactions is usually much higher than for fast neutron reactions. Fast neutrons can induce fast neutron reactions such as (n,p), (n, α), or (n,2n) which are mostly endothermic and are characterised by threshold energies. In comparison, nearly all (n, γ) reactions are exothermic and have no threshold energy to consider, which makes them the most widely used for trace element determination. [?, p.1930]

To obtain the maximum activity that can be induced, the irradiation time has to be longer (around seven times) than the half-life of the produced radionuclide. This maximum activity, A_{max} , is given by the following equation:

$$A_{max} = N\sigma\Phi \quad (8.1)$$

where N is the number of target nuclides which is related to the mass of the sample, σ is the reaction cross section (in cm^2) and Φ the neutron flux (in $\text{cm}^{-2}\text{s}^{-1}$). [?, p.1931] [?, p.1]

If the irradiation time is not that much longer than the half-life, the induced activity at the end of the irradiation can be calculated with the following equation:

$$A(t_i) = N\sigma\Phi(1 - e^{-\lambda t_i}) \quad (8.2)$$

where $A(t_i)$ is the activity after irradiation (in Bq or disintegrations per second), N is the number of target nuclides, σ the reaction cross section (in cm^2), Φ the neutron flux (in $\text{cm}^{-2}\text{s}^{-1}$), λ the decay constant (in s^{-1}) and t_i the irradiation time (in s). This equation shows that the rate of activation induced in a foil is the same as the rate of decay after

irradiation. [?, p.1931] [?, p.2]

Since the reactor neutron flux usually is not absolutely stable, comparator standards are being used to correct for these variations in the flux. The standards have well known properties and are irradiated together with the sample. They can be used to calculate the flux during the irradiation as well as correct a series of identical irradiations for flux variations. [?, p.1931]

The sample preparation is usually very easy because mostly its just packing the sample into an irradiation container. Such a container can be made of any material that is practically 'invisible' for neutrons like for instance quartz, polyethylene or aluminium. Another interesting material for a container or just for wrapping up the sample is cadmium. Cadmium has a particularly high reaction cross section for thermal neutrons which falls off rapidly in epithermal neutron sections. Putting a sample in container made of cadmium therefore shields the sample of thermal neutrons and enhances the epithermal or resonance neutron reactions. Another material used for this purpose is boron in the form of boron carbide or boron nitride. [?, p.1932]

Depending on the half-life of the radionuclide of interest, the sample is usually left to decay for some time after irradiation which is the so-called cooling down period. It allows unwanted radionuclides with a short half-life and therefore a high activity to decay before taking out and handling the sample. After that the gamma ray spectrum of the sample is recorded and analysed. [?, p.1932]

8.2 Foil Activation for Determination of the Neutron Flux

In the case of neutron flux characterization, so-called activation foils which are metallic discs, act as neutron detectors. Some of the advantages of such foils are their reliability and convenience, their small size and usability over a wide range of flux levels. [?, p.1]

As can be seen in eq. ?? the activity of a foil is dependent on the number of atoms in the foil, corresponding of course to its mass and dimensions, on the cross section of the desired nuclear reaction and on the neutron flux. Rewriting this equation results in:

$$\Phi = \frac{A_{max}}{N\sigma} \quad (8.3)$$

As explained above, A_{max} is the maximum induced activity. Since it is usually not possible to irradiate until this maximum is reached, the activity can be extrapolated to this point. This activity is the calculated maximum activity and is called saturated activity, A_{sat} . It can be calculated with the following equation:

$$A_{sat} = \frac{A_0}{(1 - e^{-\lambda t_i})} \quad (8.4)$$

where A_0 is the activity directly after irradiation, t_i is the irradiation time and λ is the decay constant. [?, p.1] [?, p.27ff]

The activity directly after irradiation can be calculated using the following equation:

$$A_0 = A(t_d) \cdot e^{-\lambda t_d} \quad (8.5)$$

where $A(t_d)$ is the activity after cooling down, t_d the cooling down period after irradiation, i.e. the time between the end of the irradiation and the measurement, and λ denotes the decay constant.

Thus, the equation for the calculation of saturated activity can also be written as:

$$A_{sat} = A(t_d) \frac{e^{-\lambda t_d}}{(1 - e^{-\lambda t_i})} \quad (8.6)$$

The neutron energy spectrum refers to the energy distribution of neutrons inside the reactor. As mentioned earlier, they are produced with high energies and then slowed down to thermal energies by the moderator. That means that the neutron energies spread over a wide energy region. Activation of a foil can occur through three different processes: absorption of thermal neutrons, resonance absorption of neutrons with intermediate or epithermal energies and threshold activation with epithermal and fast neutrons. [?, p.1f]

Thermal flux measurements are performed using materials with a high thermal neutron cross section such as gold, indium or cobalt. Epithermal and fast neutron flux can be measured using the same materials as for thermal flux measurements but covering the foils with cadmium. As mentioned earlier, cadmium has a high cross section for thermal neutrons, especially for energies below 0.4 eV. These slow neutrons are absorbed and only the neutrons with intermediate or high energies can pass through to activate the foil. The absorption cross section of cadmium can be seen in figure ???. The comparison between thermal and fast flux is called fast-to-thermal flux and can be measured if a bare and a cadmium covered foil of the same sort are activated together and their resulting activities are compared. [?, p.3]

8.2 Foil Activation for Determination of the Neutron Flux

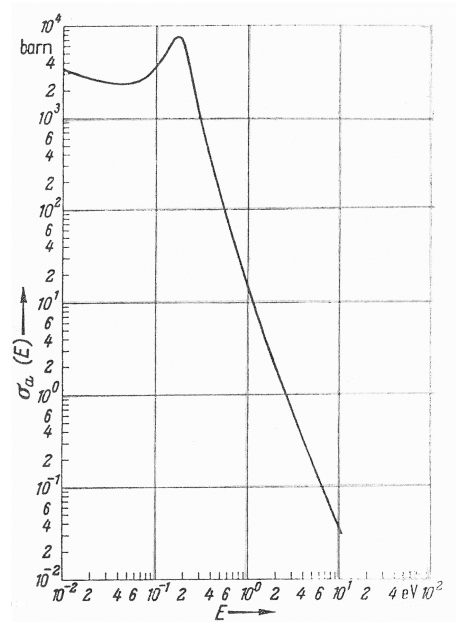


Figure 8.2: Absorption cross section of cadmium as a function of the neutron energy [?, p.273]

9 The TRIGA Mark II Reactor

The only research reactor in Austria is the TRIGA Mark II reactor at the Atominstitut (ATI) of the Vienna University of Technology. The abbreviation TRIGA stands for 'Training, Research, Isotope Production, General Atomic'. This reactor type was developed in the 1960s by General Atomic (GA) to provide a reactor with inherent safety features which could be used for training, research and isotope production. The specific designs of the TRIGA reactors vary from Mark I, Mark II and Mark III. [?, p.10] [?, p.11] [?]

The TRIGA Mark II reactor at the Atominstitut in Vienna was built by General Atomics during the years 1959 to 1962 and reached its first criticality on the 7th of March 1962. It is a pool-type research reactor above ground which uses light water as a moderator and coolant. [?, p.10]

The reactor is licensed for a maximum power of 250 kW steady state and pulse operation with up to 250 MW. The produced thermal heat is absorbed in the primary coolant circuit (de-ionised and distilled water with a temperature from 20°C to 40°C) and with a heat exchanger transferred to the secondary coolant circuit (well water with a temperature between 12°C and 18°C) and finally released into the river Danube. [?, p.10] [?, p.13]

The reactor core consists of 76 stainless steel clad zirconium-hydride fuel elements, which are arranged in an annular gridplate. Two of these 76 fuel elements contain three thermal elements, each of those is used to monitor the fuel temperature. At the maximum power of 250 kW the fuel temperature is in the area of 200°C. [?, p.10] [?, p.13]

A single fuel element has cylindrical geometry, is 3.75 cm in diameter and has a length of 72.06 cm. The cladding is stainless steel. Inside the cladding there is an active part with the actual fuel, which is 38.1 cm in length, two graphite reflectors above and below the fuel and burnable poison in form of a molybdenum disc. A schematic display of such a fuel element can be seen in figure ???. The fuel is a homogeneous metallic alloy of 8%-wt. uranium, 1%-wt. hydrogen, and 91%-wt. zirconium. The uranium enrichment is around 20%-wt.. The zirconium-hydride acts as a moderator with the favourable quality that the moderating effect decreases with increasing temperature. This property is called a negative temperature coefficient and is crucial for the inherent safety of the reactor. [?, p.10] [?, p.13] [?, p.3]

The reactor is controlled by means of three control rods which contain boron carbide as

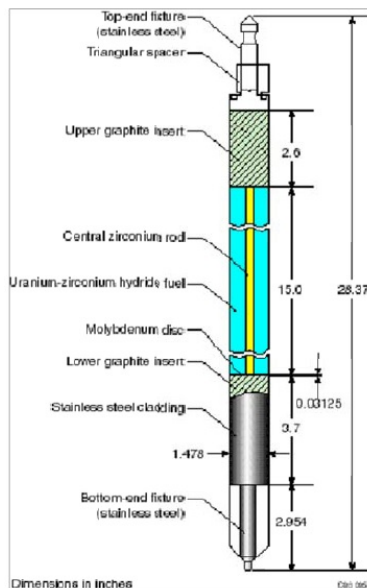


Figure 9.1: Fuel element used in the TRIGA Mark II reactor at the Atominstitut [?, p.3]

a neutron absorber. Two of the control rods are operated with an electric motor and one pneumatically. A neutron source inside the core perpetually emits neutrons. When all three control rods are inserted in the core, these neutrons are absorbed and the reactor remains subcritical. Removing the control rods from the core allows the fission process to increase and therefore the power to grow. The reactor can be shut down by inserting the control rods manually or by the reactor safety system. [?, p.10f]

The reactor power is monitored by four measuring channels. The NM-1000 is an automatic wide range channel which uses a fission chamber as a sensor, the NMP-Ph and NMP-Ch are two independent linear channels which use compensated ionisation chambers as sensors, and to monitor pulse operation there is another uncompensated ionisation chamber. [?, p.10f]

Fitting for a research reactor, the TRIGA Mark II is equipped with a number of irradiation facilities for neutron and gamma irradiation, sample activation, and isotope production. There are a central irradiation channel in the centre of the reactor core, five irradiation channels in the graphite reflector, two pneumatic transfer systems, 4 beam tubes, a thermal column and a neutron radiography facility. [?, p.10]

In figure ?? and figure ?? there are schematic displays of the vertical and horizontal section of the reactor respectively. All the above mentioned properties and facilities are displayed in these figures. [?, p.16]

Figure ?? shows the configuration of the reactor core. The 76 fuel elements are indicated by red circles, the three control rods are shown in black, the neutron source element can be found in position F25 and there are 8 dummy graphite elements in the F-ring which are

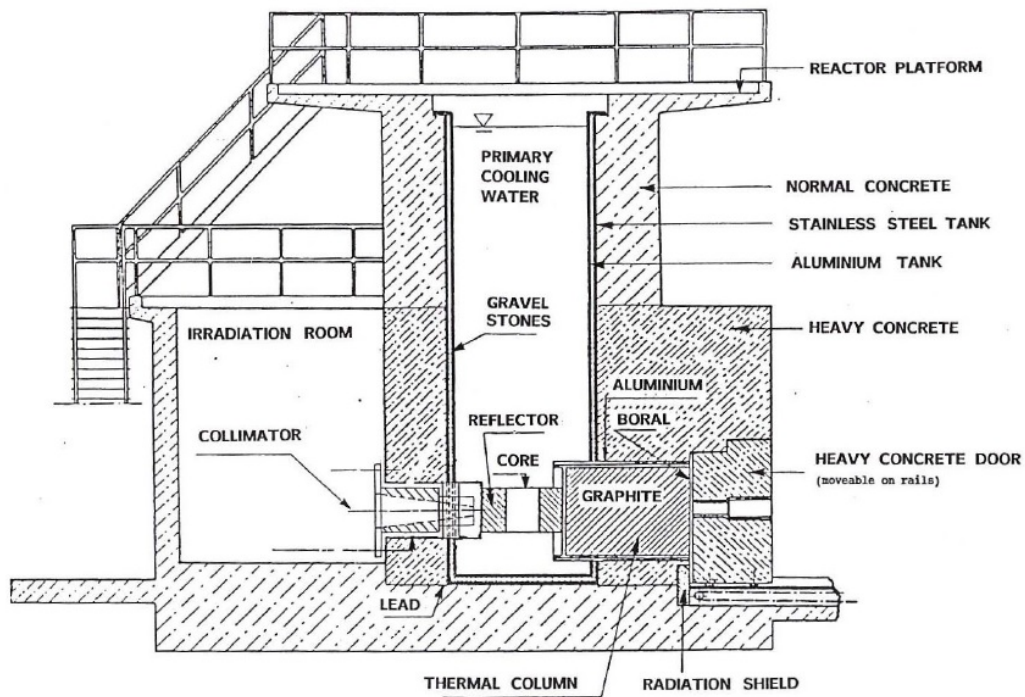


Figure 9.2: Illustration of the vertical section of the TRIGA Mark II reactor at the Atominstitut [?, p.16]

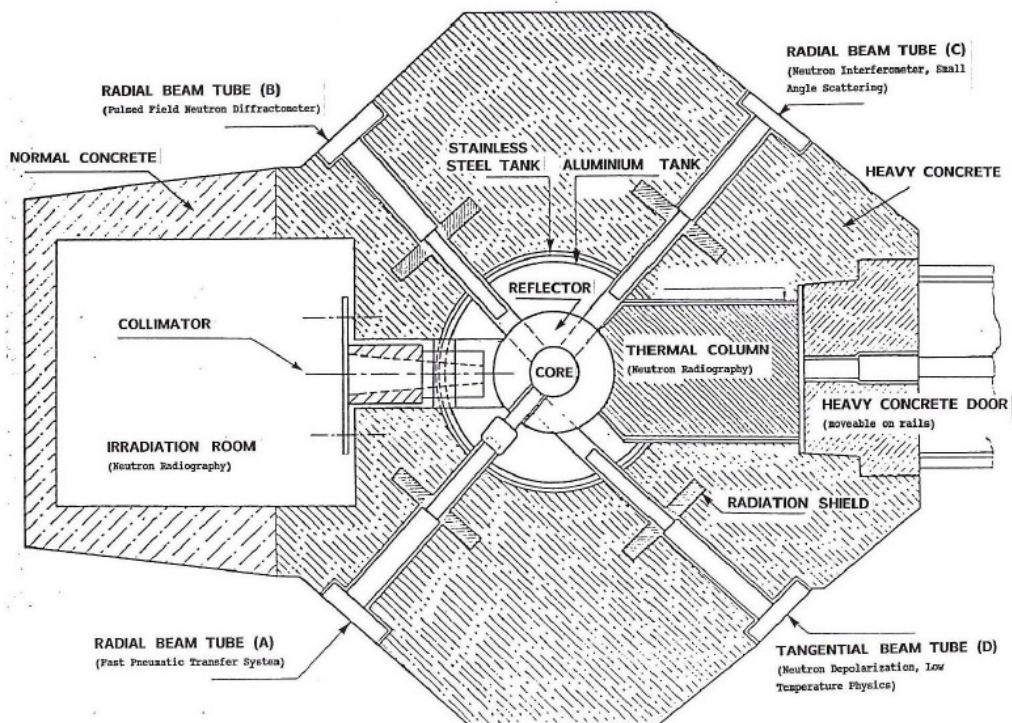


Figure 9.3: Illustration of the horizontal section of the TRIGA Mark II reactor at the Atominstitut [?, p.16]

colourless. The irradiation facilities inside the core are the central irradiation channel in green in the middle and the pneumatic transfer systems in the positions F08 and F11. [?]

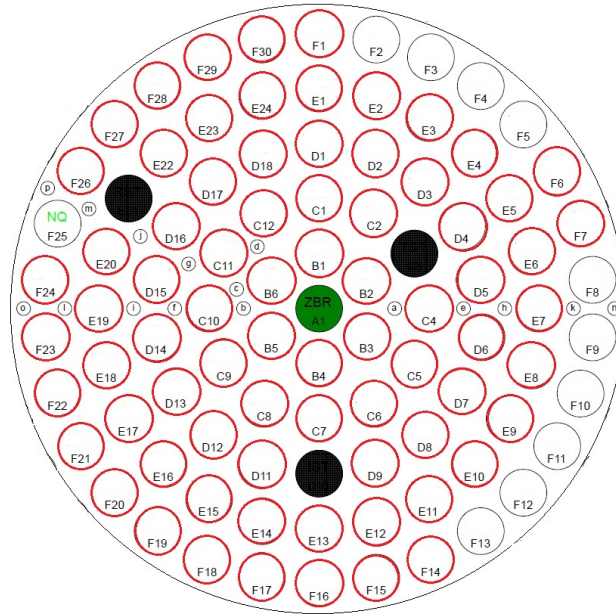


Figure 9.4: Illustration of the core configuration of the TRIGA Mark II reactor at the Atominstitut; displaying the fuel elements (red), control rods (black), and the central irradiation channel (ZBR)(green) [?, p.3]

10 Data Analysis: Gamma Spectroscopy - Detector and Software

10.1 Basics of Semiconductor Detectors

A crystalline semiconductor, most commonly silicon or germanium, is used for energy measurements, to detect charged particles and perform gamma spectroscopy. The underlying principle is that ionising radiation creates electron-hole pairs when passing through the semiconductor material. These electrons and holes are collected by an electric field. [?, p.207]

10.1.1 Basic Principle of Semiconductors

Semiconducting materials are characterised by an energy band structure consisting of a conduction band and a valence band with a relatively small energy gap in between. In figure ?? the difference between the energy band structures of semiconductors and insulators or conductors are displayed. The energy bands are caused by the close and periodic atomic structure in semiconducting crystals. At 0 K the electrons in the valence band are bound to the atoms whereas the electrons in the conduction band are free to move around in the crystal. However, at higher temperatures an electron in the valence band can be excited into the conduction band creating a hole in its initial position. This hole can be seen as positive with regard to the many electrons in the valence band. Therefore it is easy for a neighbouring electron to fill this recent hole, which leaves another hole in its turn. Continuing this sequence looks as if the hole travelled through the crystal. Thus, in a semiconducting material there are two sources of electric current which are the moving electrons in the conduction band and the moving holes in the valence band. [?, p.208f]

Assuming that the semiconductor crystal is not affected by impurities and therefore pure or 'intrinsic', there are an equal number of electrons in the conduction band and holes in the valence band. If impurities are introduced into the crystal, a 'doped' or 'extrinsic' semiconductor is created. Silicon and germanium are both tetravalent atoms and can be doped by either pentavalent or trivalent atoms, depending on in which direction one wants to tilt the balance. In figure ?? one can see the crystal lattice of tetravalent atoms which contains impurities. The effects of those impurities will be discussed briefly below. [?, p.209]

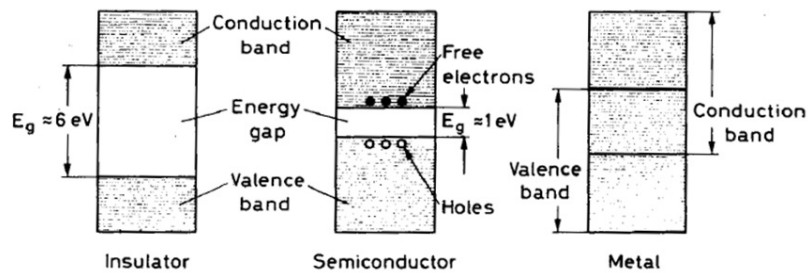


Figure 10.1: Illustration of the energy band structure of semiconductors, insulators and conductors [?, p.208]

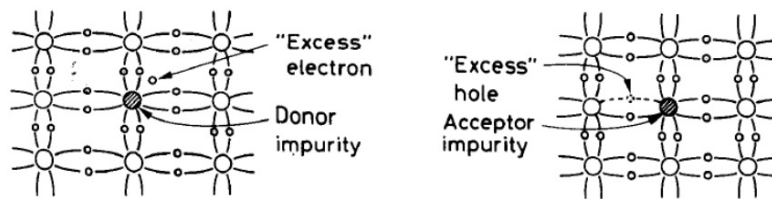


Figure 10.2: Schematic display of the atomic lattice of a doped tetraivalent semiconductor such as silicon or germanium [?, p.212]

With pentavalent impurity atoms in an otherwise tetraivalent crystal there are extra electrons which do not fit into the valence band. Thus such impurities are called donor impurities. Due to the impurities a discrete energy level is created which is very close to the conduction band but strictly speaking still in the energy gap. The additional electrons reside in this extra level but can very easily be lifted into the conduction band. At normal temperatures these extra electrons will also help filling the arising holes. Having more electrons in the conduction band and less holes in the valence band, the current is a result of the moving electrons. Such semiconducting materials are referred to as n-type semiconductors. [?, p.212f]

If the impurities are trivalent the situation is more or less reversed. There is an excess of holes in the valence band making the movement of these holes the main contributor to the current. Such semiconductors are called p-type semiconductors. The atomic lattice of a doped semiconductor is schematically displayed in fig ?? [?, p.213]

10.1.2 Semiconductor Detectors

A highly important concept for the functioning of a semiconductor detector is the semiconductor junction. In electronics such junctions are also known as rectifying diodes. A p-type and n-type semiconductor are placed in juxtaposition, thus creating a pn-junction. The region between those two materials will become electrically charged due to the diffusion of

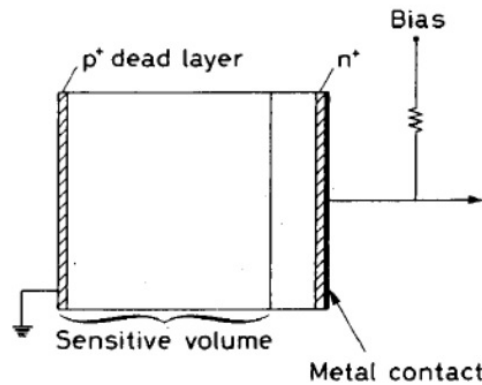


Figure 10.3: Basic configuration of a semiconductor junction used as a radiation detector [?, p.220]

electrons towards the p-type material and the diffusion of the holes into the n-type semiconductor. This electric field creates a so-called contact potential. This described zone is called depletion zone due to the fact that there are no mobile charge carriers in that area. The electric field immediately sweeps out any entering electron or hole. This effect is used to detect ionising radiation. [?, p.215]

Incoming radiation creates electron-hole pairs which are collected by the electric field. Placing electrical contacts on either end of the semiconductor junction makes it possible to detect a current signal which is proportional to the ionisation. [?, p.216]

An important factor is the depletion depth, which is the width of the depletion zone. Usually this zone is quite small. But since it depends on the impurity concentration it can be broadened by doping one side more heavily than the other, thus extending the depletion zone into the lighter doped side. [?, p.216]

To further increase the width of the depletion zone and to decrease noise effects in the output signal, a reverse-bias voltage is applied to the junction. Applying a positive voltage to the n-type side of the junction will attract the electrons in the n-region towards this contact and away from the junction. Of course this works for the holes in the p-side accordingly. [?, p.218]

In figure ?? the basic configuration of a semiconductor junction functioning as a radiation detector is laid out. The collection of the charges which are produced by the passage of ionising radiation is accomplished by fitting an electrode on either end of the junction. To prevent the formation of a rectifying diode when bringing the metal in contact with the semiconductor, there are heavily doped n^+ and p^+ materials in between. [?, p.219f]

A series resistor supplies the bias voltage to the detector and a charge-sensitive preamplifier collects the charge signal from the detector. After the preamplifier the signal is processed and optimized. [?, p.220]

10.1.3 Germanium Detectors

For detection of gamma rays the preferred semiconductor material is germanium. It has a higher atomic number and therefore a greater photoelectric cross-section than silicon. A small disadvantage is that due to the smaller energy band gap it has to be operated at low temperatures and therefore constantly cooled. The greater efficiency however compensates for this inconvenience. [?, p.231]

At first the gamma-detectors were made from lithium compensated germanium, so-called Ge(Li) detectors. A disadvantage of these detectors is that they have to be cooled to liquid nitrogen temperatures at all times due to the high mobility of the lithium atoms. A more recent development are high purity germanium (HPGe) detectors. These use intrinsic germanium with very low impurity concentrations in the order of 10^{10} atoms/cm³. [?, p.231f]

10.2 Gamma Spectroscopy

Germanium detectors are primarily used to perform gamma ray spectroscopy. They have the highest energy resolution for gamma rays in the range from a few keV up to 10 MeV. To reduce the signal to noise ratio, the detector has to be shielded with lead. [?, p.233]

A most important matter is the calibration of the absolute detection efficiency. It is necessary to be able to measure absolute intensities. A calibration is performed with a gamma source which spans over the desired energy region. Usually one considers the full peak efficiency, which is the efficiency for a photoelectric conversion. To obtain this efficiency the total count rate for each gamma photo peak is divided by the total output. [?, p.233]

The geometry in which the calibration source is measured is very important for the possibility of future use of a calibration. The size and geometry of the calibration source should be very much like the size and geometry of the sample, although a point-like geometry can be assumed in case of most commercial calibration sources. Furthermore, the distance between source and detector should be reproducible. Therefore it is useful to use a specific sample holder for the calibration and for the measurements. [?, p.233f]

As discussed in Section ??, the dead time plays an important role during a measurement. Additionally, summing effects can arise which is why the count rate should be kept at reasonable levels. [?, p.234]

11 Laboratory Equipment

11.1 Detector

The detector which was used for the measurements in the course of this master thesis was provided by the radiation protection group. It was a low level detector identified by the name of "Wufti".

It was a coaxial closed-ended high purity germanium n-type detector by Canberra (series GC5020) which was cooled with liquid nitrogen. The relevant information can be found in table ?? . The 'detector specification and performance data' sheet in the appendix provides further information.

Model	GC5020
Geometry	Coaxial one open end, closed end facing window
Crystal diameter	65 mm
Crystal length	68 mm
Relative efficiency	58.2%
FWHM at 122 keV (^{57}Co)	0.980 keV
FWHM at 1.33 MeV (^{60}Co)	1.81 keV
Peak/Compton ratio	73.6:1

Table 11.1: Characteristics of the detector used in the course of this work (for more detailed information see data sheet in the appendix)

As a standard feature the detector is shielded with –starting from the outside– around 12 cm of lead, 1 mm cadmium or zinc and 2 mm copper. The additional layers are necessary because when lead absorbs an ionising particle it subsequently emits X-rays. The zinc atoms absorb the X-rays from the lead but also emit X-rays with lower energies which are absorbed by the copper. The X-rays that are emitted by copper are of very low energies and do not influence the detector. Additionally to the standard shielding, the detector was shielded with 5 cm lead bricks. In figure ?? and figure ?? there are pictures of the detector inside and its shielding respectively.



Figure 11.1: Gamma detector with additional shielding and liquid nitrogen cooling

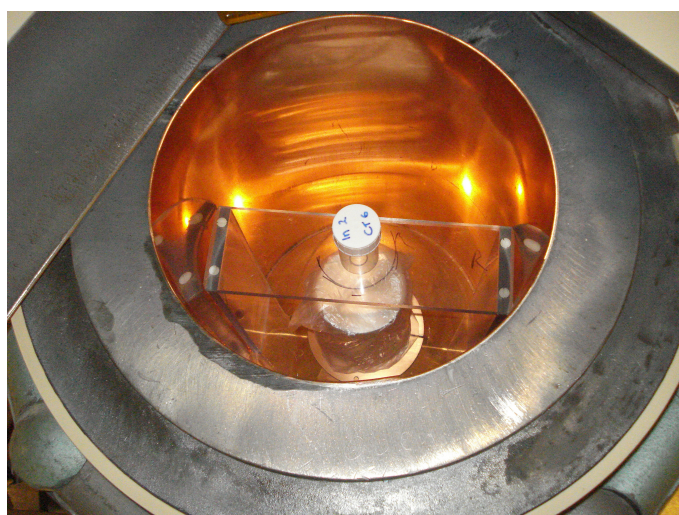


Figure 11.2: Inside of the gamma detector in a typical measurement configuration

11.2 Software

In order to process and analyse the data obtained by the detector, complementary software is needed. The software which was used in the course of this work was 'Genie™ 2000 Spectroscopy Software', developed and sold by Canberra Industries Inc.

As stated in the Operations Manual provided by Canberra, "Genie 2000 is a comprehensive set of capabilities for acquiring and analyzing spectra from Multichannel Analyzers (MCAs). Its functions include MCA control, spectral display and manipulation, basic spectrum analysis and reporting." [?, p.1]

The analysis of a gained spectrum is simplified by nuclide identification, which matches the energies of the measured full energy peaks by use of a nuclide library to the corresponding nuclides. The peak areas and their errors are identified by the software and are being used in further consequence to calculate the activities of the respective nuclides. [?]

11.3 Calibration

In order to acquire useful data the detector-software system has to be calibrated. Since the materials and dimensions of the samples were known beforehand, the calibration was performed using a calibration standard of corresponding geometry. It was a certified solid multi gamma calibration source manufactured by Eckert & Ziegler Nuclitec GmbH (Type QCRB1186). The contained nuclides and their photo peak energies are displayed in table ?? . The data sheet including further information can be found in the appendix.

11.3.1 Energy Calibration

As explained in the Genie 2000 Tutorials: "Energy calibration establishes a linear relationship between the spectrum's channels and their energy levels. By calibrating two peaks, one at each end of the spectrum, the energy of any other peak can be estimated fairly accurately." [?, p.21]

The calibration source is placed within a well defined distance from the detector and a spectrum is recorded. With the information about the nuclides, peak energies and activities contained in the certificate provided by the manufacturer, a certificate file is created. The software then calculates a calibration polynomial of the form

$$E = C_0 + C_1 \cdot x + C_2 \cdot x^2 + C_3 \cdot x^3 \quad (11.1)$$

Nuclide	Photo peak energy [keV]
Americium-241	60
Cadmium-109	88
Cobalt-57	122
Cerium-139	166
Mercury-203	279
Tin-113	392
Strontium-85	514
Caesium-137	662
Yttrium-88	898
Cobalt-60	1173
Cobalt-60	1333
Yttrium-88	1836

Table 11.2: List of nuclides and their photo peak energies contained in the certified calibration source from Eckert & Ziegler

where x gives the channel number and C_0 , C_1 , C_2 , and C_3 are the coefficients that have to be determined. Those coefficients represent the energy offset, the 'gain' and they take the non-linearity of the system into account. [?, p.254]

11.3.2 Efficiency Calibration

The efficiency of a detector changes with different gamma ray energies. An efficiency calibration compensates that effect and is necessary to determine the correct activity of a sample. It also takes the source-detector geometry into account. [?, p.25f]

After taking a spectrum of the calibration source in a defined geometry, the certificate file is used to calculate an efficiency curve. To get a better fitting overall curve it is also possible to use a combination of two curves, the dual polynomial curve. In the course of the calibration, the cross over energy where those two curves meet is defined by the user. In our case the cross over point was at 122 keV, which separates the low from the high energy region. [?, p.25f]

The efficiency curve can be written as a polynomial function of the form

$$\ln(\varepsilon) = \sum_{i=0}^n b_i (\ln(E))^i \quad (11.2)$$

where ε is the efficiency at the photo peak energy, E , and b_i are the coefficients that have to

be determined. [?, p.258]

For this work efficiency calibration files using dual polynomial curves for various reproducible source-detector geometries were created. In the end, only two geometries were used in all the measurements which was a small table with a distance of about 2 cm from the crystal and a medium table with a distance of 9 cm from the crystal. A typical measurement configuration with the medium table and one of the samples on top can also be seen in figure ??.

The energy calibration curve for the small table is shown in figure ?. The efficiency calibration curves with linear and logarithmic scale are depicted in figure ?? and figure ?? respectively.

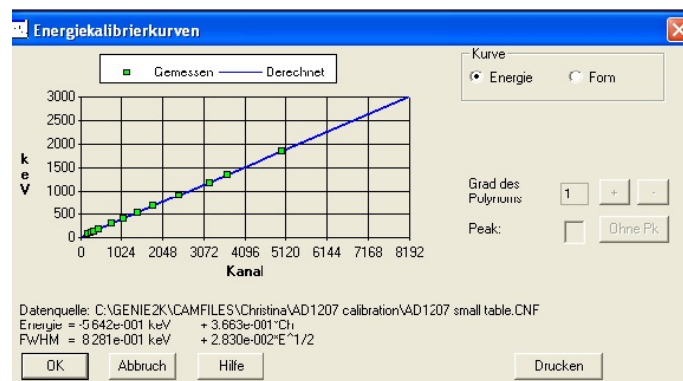


Figure 11.3: Energy calibration curve for the small measuring table

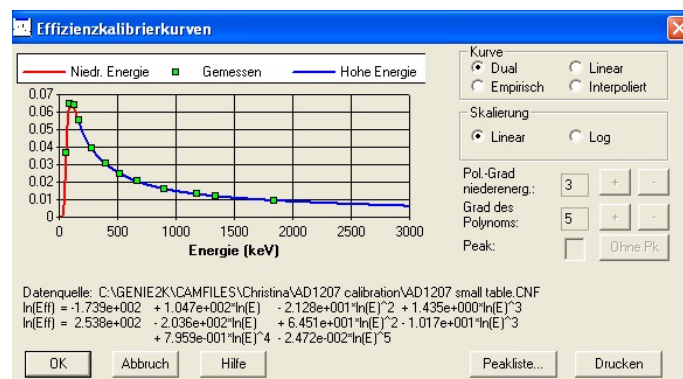


Figure 11.4: Efficiency calibration curve for the small measuring table (linear scale)

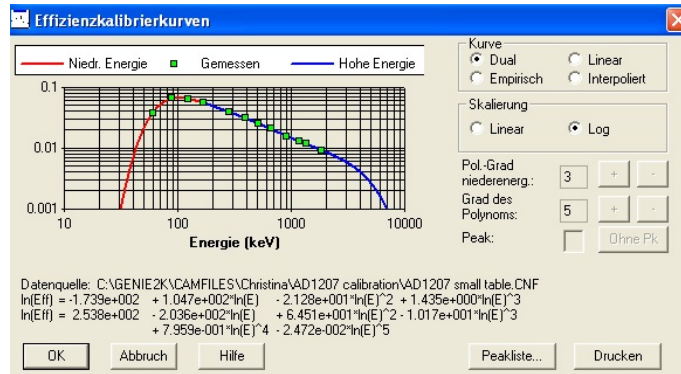


Figure 11.5: Efficiency calibration curve for the small measuring table (logarithmic scale)

For the medium table the energy calibration curve is depicted in figure ???. The efficiency calibration curves with linear and logarithmic scale can be found in figure ??? and figure ??? respectively.

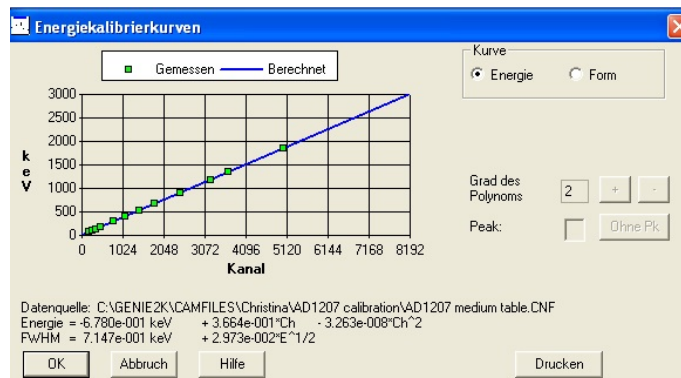


Figure 11.6: Energy calibration curve for the medium measuring table

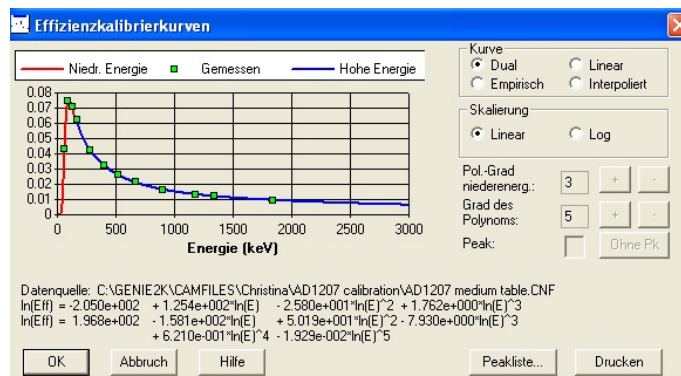


Figure 11.7: Efficiency calibration curve for the medium measuring table (linear scale)

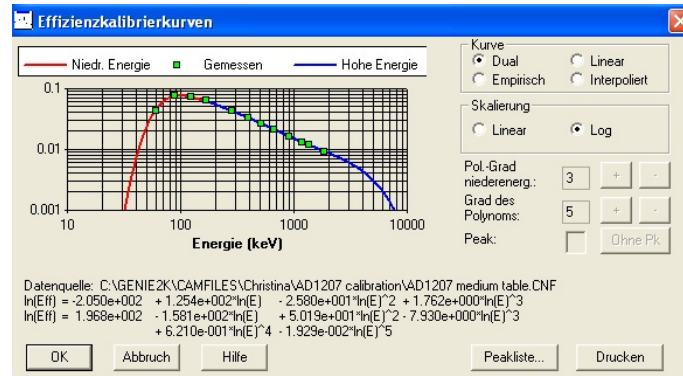


Figure 11.8: Efficiency calibration curve for the medium measuring table (logarithmic scale)

12 Experimental

Neutron activation analysis measurements were performed using foils of various materials in different positions inside the TRIGA Mark II reactor at the Atominstitut of the Vienna University of Technology. The irradiations of the foils were planned and conducted with the objective to detect certain reactions which would help to characterise the neutron spectrum. The measurements were performed using gamma ray spectroscopy. From the measured values the saturated activities were calculated and corrected for flux variations.

12.1 Reactions

For the purpose of determining the neutron energy spectrum, foils of different nuclides and reactions were selected. Some of the reactions were (n,p) threshold reactions which can only take place when the neutron energies are high enough. The various nuclides and reactions plus the threshold energies of the reactions, the cross sections and the half-lives of the product nuclides, can be found in table ??

Nuclide	Reaction	Threshold energy [MeV]	Cross section [cm ²]	Half-life
¹⁹⁷ Au	¹⁹⁷ Au(n,γ) ¹⁹⁸ Au	-	98.8 · 10 ⁻²⁴	2.7 d
⁶³ Cu	⁶³ Cu(n,γ) ⁶⁴ Cu	-	4.5 · 10 ⁻²⁴	12.7 h
¹¹⁵ In	¹¹⁵ In(n,n') ¹¹⁵ In*	1.65	3.5 · 10 ⁻²⁵	4.36 h
⁵⁸ Ni	⁵⁸ Ni(n,p) ⁵⁸ Co	2.5	6 · 10 ⁻²⁵	70.78 d
⁵⁴ Fe	⁵⁴ Fe(n,p) ⁵⁴ Mn	3.75	4 · 10 ⁻²⁵	312.7 d
²⁷ Al	²⁷ Al(n,p) ²⁷ Mg	5.30	8 · 10 ⁻²⁶	9.43 min

Table 12.1: List of parent nuclides, reactions, threshold energies, cross sections and half-lives of the product nuclides

The various reactions and the decays of the products will be discussed below. All the information (in particular the decay schemes) presented below was obtained from the Chart of Nuclides database of the National Nuclear Data Center, see [?].

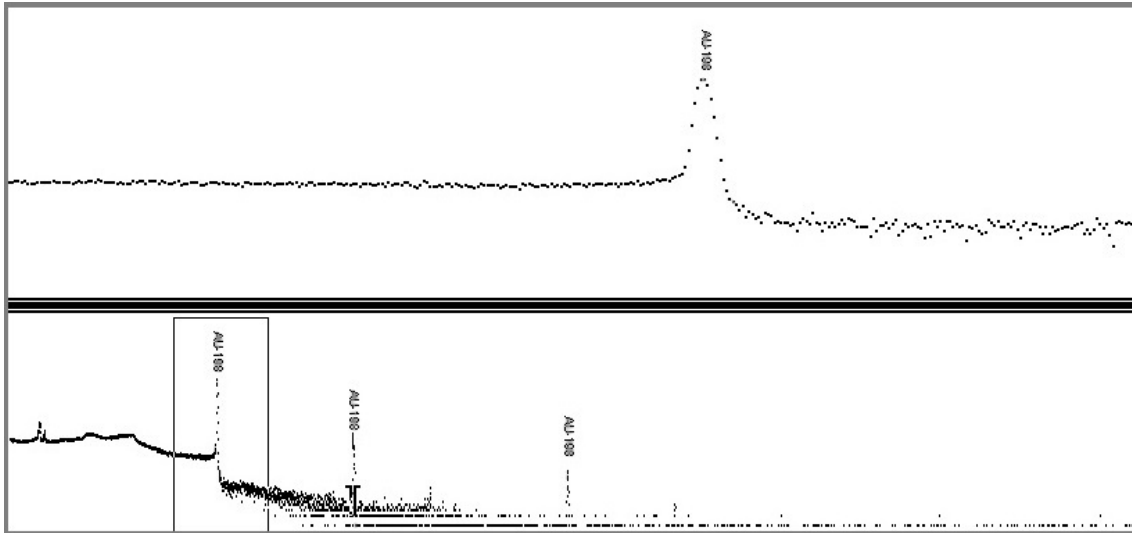


Figure 12.1: Typical gamma spectrum of an activated gold foil

$^{197}\text{Au}(n,\gamma)^{198}\text{Au}$

The product of this (n,γ) reaction of ^{197}Au is ^{198}Au , which can decay either by emission of a β^- -particle with a half-life of 2.6948 d or if it is in an excited energy level by isomeric transition with a half-life of 2.272 d. The decay of interest was the β^- -decay to ^{198}Hg . The decay scheme of this decay is illustrated in figure ???. The gamma ray energies are displayed in blue in keV with their intensities next to them. Noticeably, the 411.8 keV line has the highest intensity and is therefore the easiest to detect and measure without much difficulty or uncertainty.

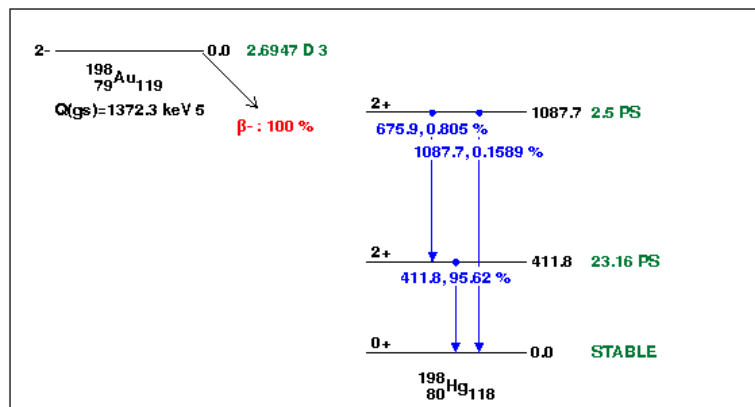


Figure 12.2: Decay scheme of ^{198}Au

In figure ??? a typical gamma spectrum of an activated gold foil can be seen. This particular screenshot was taken from the measurement of a gold foil which was irradiated in the first position in the horizontal beam tube. The reactor power was 10 kW and the irradiation time

30 min. The counting time in this case was 25 min. The upper part of the window contains a close-up view of the 411.8 keV gamma peak. The shape of this particular peak is very well defined and it looks pretty much like a textbook example. The lower window depicts the overall gamma spectrum. The 411.8 keV peak is the particularly high one with the frame around it, the 675.9 keV and 1087.2 keV peaks are also visible next to it.

$^{63}\text{Cu}(n,\gamma)^{64}\text{Cu}$

The product of the (n,γ) reaction with ^{63}Cu is ^{64}Cu , which decays with a half-life of 12.701 h. To 38.50% the decay takes place via emission of a β^- -particle and to 61.50% the decay mode is a combination of electron capture and β^+ -decay. The latter of those was the one of interest. The decay scheme of the transformation to ^{64}Ni can be found in figure ???. This decay is characterised by a gamma energy peak at 1345.8 keV.

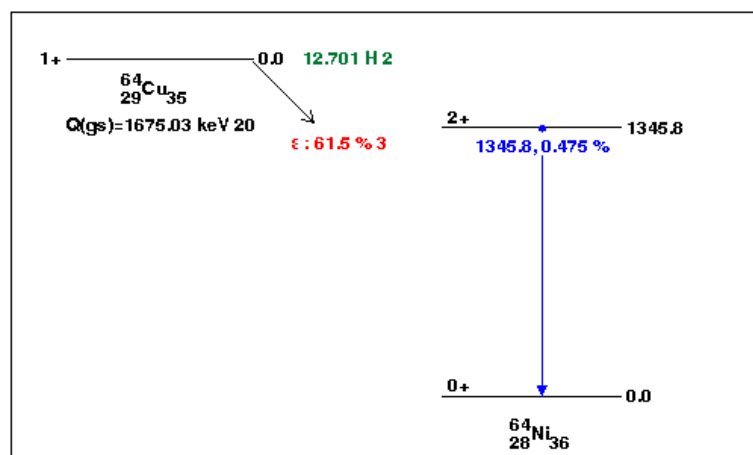
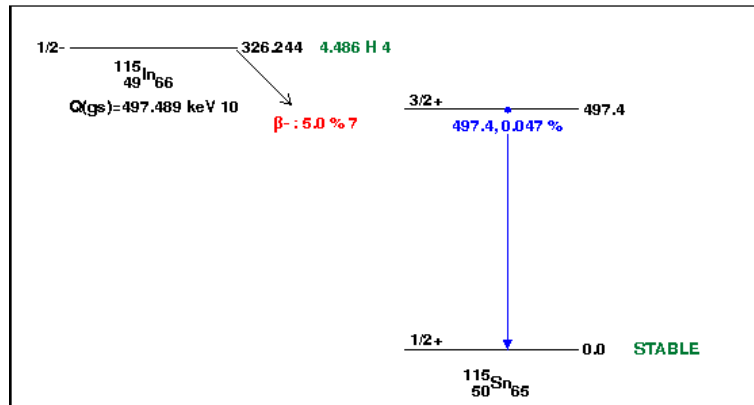


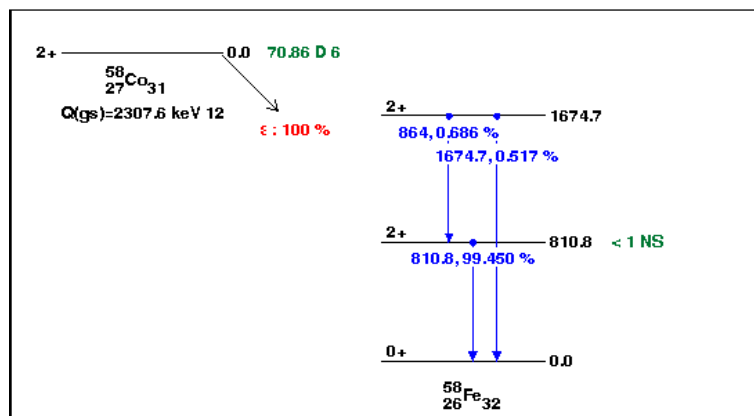
Figure 12.3: Decay scheme of ^{64}Cu

$^{115}\text{In}(n,n')^{115}\text{In}^*$

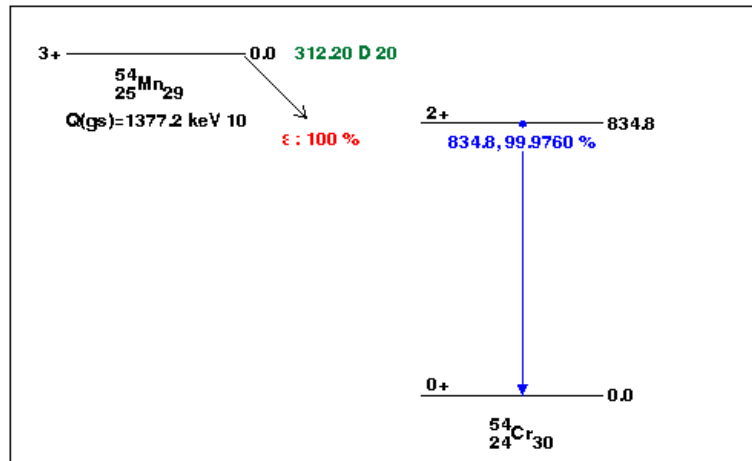
The $^{115}\text{In}^*$ that is produced in the (n,n') reaction with ^{115}In is in an excited state and decays with a half-life of 4.486 h into ^{115}Sn . The decay mode is mostly (95%) isomeric transition. However, the β^- -decay with only 5% probability was the one of interest for this work. The decay scheme with the characteristic 497.4 keV energy line is displayed in figure ???. It is important to note that this is a threshold reaction which takes place only when the neutron energy is higher than 1.65 MeV.

Figure 12.4: Decay scheme of $^{115}\text{In}^*$ $^{58}\text{Ni}(n,p)^{58}\text{Co}$

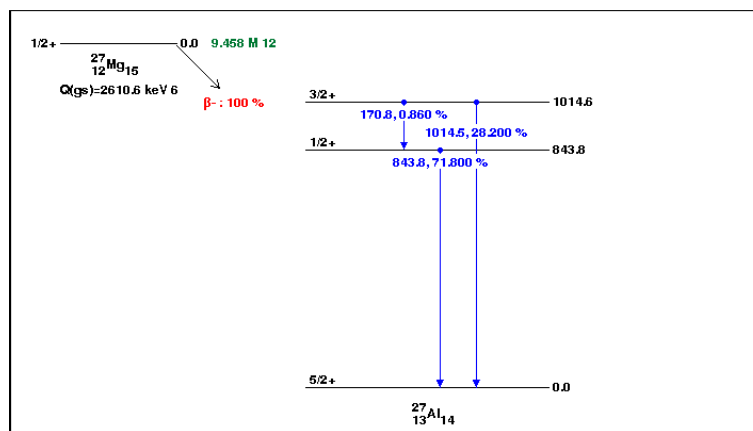
The (n,p) reaction of ^{58}Ni to ^{58}Co is a threshold reaction with a threshold energy of 2.5 MeV. The product decays with a half-life of 70.86 d via a combination of electron capture and β^+ -decay to ^{58}Fe . The decay scheme can be seen in figure ???. This decay can be detected via various energy peaks in the gamma spectrum. The one with the highest intensity is at 810.8 keV.

Figure 12.5: Decay scheme of ^{58}Co $^{54}\text{Fe}(n,p)^{54}\text{Mn}$

Another threshold reaction with a threshold energy of 3.75 MeV, is the (n,p) reaction of ^{54}Fe to ^{54}Mn . The manganese has a very long half-life of 312.12 d and decays via a combination of electron capture and β^+ -decay to ^{54}Cr . Figure ?? shows the decay scheme of this decay. There is only one possible gamma energy line, by which this decay can be detected, and that one is at 834.8 keV.

Figure 12.6: Decay scheme of ^{54}Mn $^{27}\text{Al}(n,p)^{27}\text{Mg}$

The reaction with the highest threshold of 5.30 MeV was the (n,p) reaction of ^{27}Al to ^{27}Mg . The magnesium decays with a comparatively short half-life of 9.458 min via β^- -decay back to ^{27}Al . The decay scheme of this decay can be found in figure ???. The gamma energies by which this decay can be measured are 170.8 keV, 843.8 keV and 1014 keV.

Figure 12.7: Decay scheme of ^{27}Mg

12.2 Foils

Since the materials were all solid metals, the easiest geometry for the samples was to be in the form of foils. In order to achieve a reasonable activation with comparatively short irradiation times (meaning around half an hour), it was important to have a sufficient number of atoms in the sample. The term 'atoms' here only refers to atoms of the type of nuclide that was of interest. Thus, in this consideration the isotopic abundance of an element had to be taken into account.

In the end, after a little research about different possibilities, round discs with a diameter of 6 mm were chosen. The thickness of the discs varied between 0.025 mm and 1 mm in order to compensate for the isotopic abundance and the difficulty of activating a certain reaction. In table ?? there is all the information concerning the foils that were used for irradiations: the element, the pureness of the foil material, the nuclide of interest, the isotopic abundance for that particular nuclide, as well as the dimensions of the discs and their (calculated) average weight.

The certificates of the foils, containing information about the specific matrix uncertainties of the geometry and impurities, can be found in the appendix.

Element	Pureness	Nuclide	Isotopic abundance	Diameter [mm]	Thickness [mm]	Mass [mg]
Au	99.99 %	^{197}Au	100 %	6	0.025	13.66
Cu	99.99 %	^{63}Cu	69.1 %	6	0.5	126.58
In	99.999 %	^{115}In	95.71 %	6	0.5	103.34
Ni	99.999 %	^{58}Ni	68.08 %	6	0.5	125.85
Fe	99.99 %	^{54}Fe	5.8 %	6	1	222.63
Al	99.99 %	^{27}Al	100 %	6	0.25	19.09

Table 12.2: Information about the activation foils used in this work: element, pureness, nuclide of interest, isotopic abundance, dimensions and weight of activation foils

The mass value in table ?? was calculated using the dimensions of the foils and the density of the element material. Therefore, those values are just to point out the general average mass of the activation foils. All the foils were weighted before they were irradiated and for further calculations this specific and exact value was used.

Cadmium Covers

As mentioned before, cadmium has a particularly high absorption cross section for low energies, which can be seen in figure ???. Thus, covering a foil with cadmium will shield the foil from thermal neutrons and activation will only be on account of epithermal and fast neutrons. The exact Cadmium cut-off energy is in fact a function of the thickness of the cadmium cover, which can be seen in figure ???

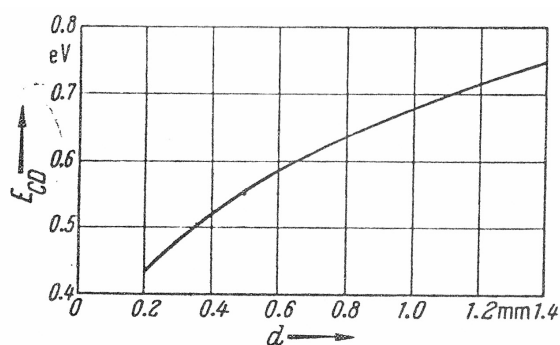


Figure 12.8: Cadmium cut-off energy as a function of the cadmium thickness [?, p.276]

The covers used were made of a cadmium sheet with a thickness of 0.5 mm. Thus the cadmium cut-off energy was at 0.55 eV, as can be seen in figure ???.

The sheet was either folded to enclose the foil in the case of the irradiations in the horizontal beam tube or made into a little cup with a fitting lid where the foil was safely contained, unable to slip out and covered from every side. The cups were used in the irradiations in the central irradiation channel. The cadmium covers with a measuring tape placed behind them to show the dimensions can be seen in figure ???.

Due to the otherwise high activation via (n,γ) reactions of other isotopes in indium, these foils were always covered with cadmium. Furthermore, there was always one bare and one cadmium-covered gold foil in the irradiations to be able to compare the activation by the total neutron flux and the activation by the epithermal and fast neutrons. Whenever a foil was cadmium-covered there will be a (Cd) next to the foil material, as for example in Au(Cd).



Figure 12.9: Cadmium covers folded and made into small cups to enclose the foil

12.3 Irradiations

In the course of this work irradiations were performed in two different irradiation facilities. A total of 14 positions was characterised. At first, irradiations were conducted in one of the horizontal beam tubes, in particular the radial beam tube B, which can be seen in figure ?? and ?. The other irradiations were performed in the central irradiation channel in the centre of the the reactor core. This position can also be seen in figure ?? and more detailed in figure ?. The details about those two positions, including the sample holders and the irradiation information, will be discussed in the following.

One set of activation foils consisted of Au, Au(Cd), Cu, In(Cd), Ni, Fe, and Al. The additional '(Cd)' next to the element indicates that the foil was covered with cadmium during irradiation.

12.3.1 Horizontal Beam Tube

The horizontal beam tubes at the TRIGA Mark II reactor at the Atominstitut are usually all used for various ongoing experiments of the different research groups. But due to inspections and modifications on the radial beam tube B, it was available for irradiations. For nearly all experiments the neutron beam is collimated by a so-called collimator which lies inside the beam tube. The collimator from the beam tube B was taken out for inspection and therefore the tube was empty and accessible all the way to the reflector. Since this situation was of limited duration, only three irradiations in different positions could be arranged. [?]

The positions inside the tube were spread over the whole length of the tube and were characterised by their distance from the reflector, which was 5 cm for the first position, 125 cm for the second position and 185 cm for the third position. The positions can be seen in figure ?. [?, p.2]

Since it was of utmost importance to use a material that would not be activated and could be taken out a short time after irradiation, the sample holder which was used for these irradiations was made out of wood. It can be seen in figure ?. The main reason for extracting the sample holder and starting a measurement rather sooner than later was of course the ^{27}Mg with a half-life of approximately 9 min. Not being able to extract the sample holder around half an hour after irradiation would have meant losing the possibility to detect the (n,p) reaction of ^{27}Al .

For the irradiation, the foils were put into individual bags made out of paper and then hung between two wooden poles like little flags. The purpose of this was to have as little material as possible around the samples and of course also to have a material that would not interact with the foils or interfere with the neutron flux. An additional advantage of this method was

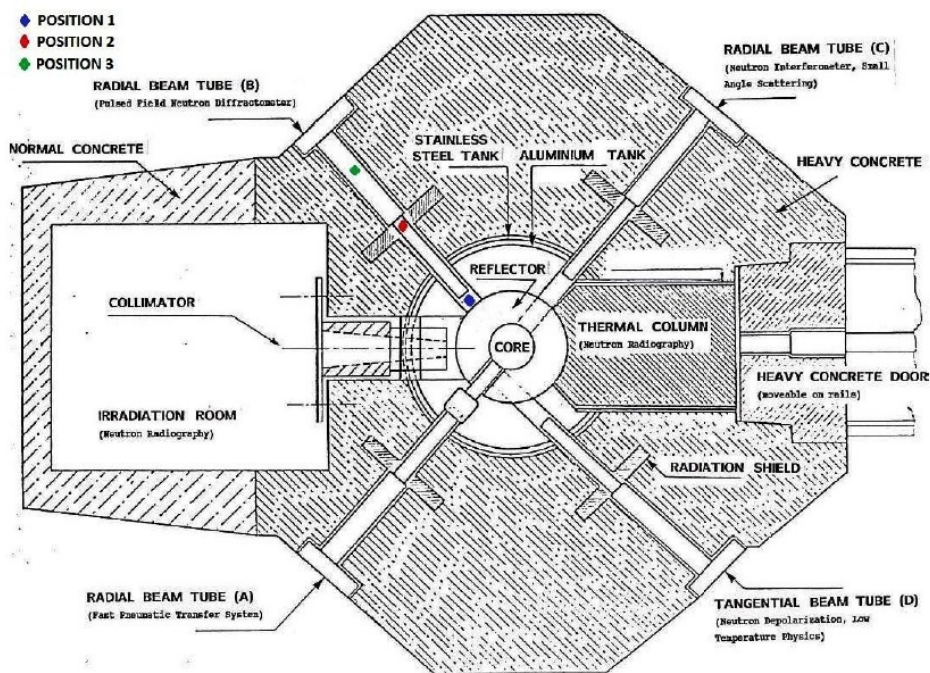


Figure 12.10: Irradiation positions in the horizontal beam tube [?, p.2]. Position 1 is 5 cm from the reflector, position 2 125 cm and position 3 185 cm.



Figure 12.11: Sample holder used for irradiations in the horizontal beam tube

that the foils could simply be cut down after extraction and cooling down. Therefore the time spent close to the radioactive material was short and the foils could be measured more quickly. In figure ?? the sample holder can be seen as it was prepared for the first irradiation position close to the reflector. The modified sample holder for the second irradiation and a close view of the suspended foils can be seen in figure ??.

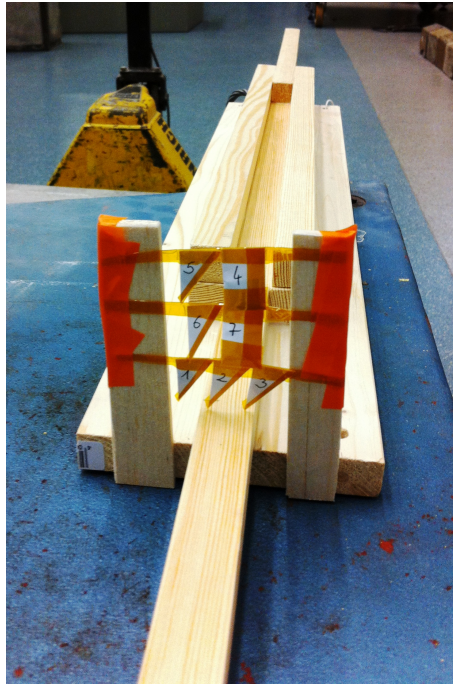


Figure 12.12: Sample holder prepared for irradiation in the second position. The foils are contained in separate paper bags and suspended between two wooden poles

In the first and second position the whole set of foils was irradiated, in the third position only three foils (Au, Au(Cd) and Cu) were used, because the irradiation power and time was limited and most of the samples would not have been activated properly under the given circumstances.

The reactor power was always 10 kW, the irradiation time was 30 min, except for the irradiation in the third position, for which the time was 60 min in order to compensate for the reduced neutron flux. The specifics of the single irradiations can be seen in table ??.

The results of the measurements and calculations for the beam tube can be found in ??.

12.3.2 Central Irradiation Channel

The central irradiation channel, or central thimble, lies in the centre of the reactor core and is surrounded by the fuel elements. The exact configuration can be seen in figure ??.

	Distance from reflector	Irradiated foils	Reactor power	Irradiation time
Position 1	5 cm	Au, Au(Cd), Cu, In(Cd), Ni, Fe, Al	10 kW	30 min
Position 2	125 cm	Au, Au(Cd), Cu, In(Cd), Ni, Fe, Al	10 kW	30 min
Position 3	185 cm	Au, Au(Cd), Cu	10 kW	60 min

Table 12.3: Irradiations performed in the horizontal beam tube

The purpose in these irradiations was to characterise the neutron flux in the centre of the reactor core along the vertical axis. To determine what the sample holder should look like and where the foils should be positioned for irradiation, a couple of previous irradiations and measurements were necessary.

Sample Holders

As mentioned earlier, a fuel element has a length of 72.06 cm with an active part of 38.1 cm in the middle between the graphite reflectors. In the appendix there are two schematic illustrations of the vertical cross section of the reactor core. Unfortunately the data given by those two references is not identical and therefore the actual dimensions were unknown.

Since the middle of the active part of a fuel element would be an interesting position to characterise, there were a few preceding irradiations to find this central position (measured from the bottom of the central irradiation channel). In order to find this position, it was assumed, that being in the exact centre would correspond to having the maximum flux and therefore maximum activation of a foil. So a couple of small gold foils with a diameter of 5 mm were spread over an aluminium sample holder with a distance of 1.5 cm between their centres. The foils were irradiated for 10 min at 100 W reactor power. After a few days of cooling down they were measured and the data evaluated. According to reactor theory the vertical neutron flux has the shape of a cosine. Therefore, a cosine was fitted to the measured and calculated values to determine the maximum of the activation and thus the centre of the reactor core. The maximum lay at 34.2 cm, measured from the bottom of the central irradiation channel. Figure ?? shows the plot of one of the measurements with the fitted cosine. Although the measured activities varied slightly in their particular value, previous irradiations supported the conclusion that the maximum given by the cosine function was correct. Thus, the centre of the core was determined to be at 34.2 cm measured from the bottom of the central irradiation channel.

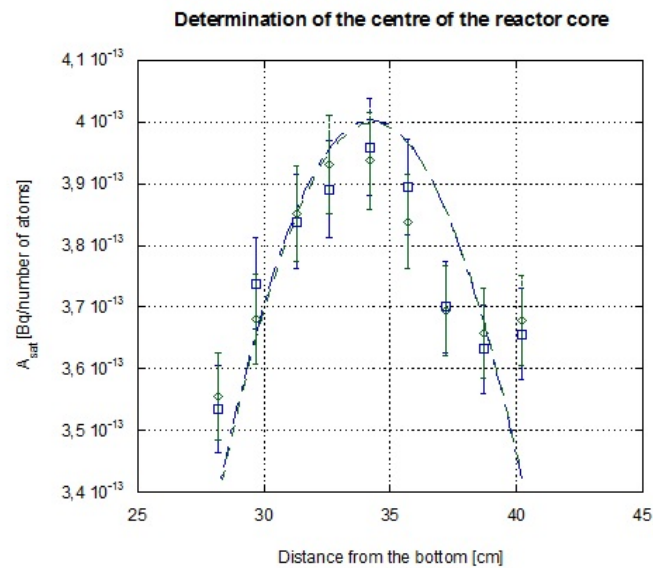


Figure 12.13: Determination of the central core position

With this information about the central position, a sample holder was designed that had one position exactly in the centre and ten others spaced equally around that position. The sample holder had a total length of 64 cm, a width of 2 cm and a thickness of 4 mm plus the cover with a thickness of 1 mm. The cover was fixed with screws made of the same material as the sample holder. The distance between the eleven sample positions was 4 cm (measured from the centres of the holes). Also a position for the reference foil was included. Such a reference foil enables corrections of the variations of the neutron flux due to power fluctuation. This reference position was in between the central and the next higher position with a distance of 2 cm to those positions.

As to the material it was decided that aluminium would be best for all irradiations except aluminium itself. Aluminium as the sample holder material had the advantages of minimal interference with the neutron flux and a short half-life of its activation products. The short half-life was essential because it reduced the cooling down period before the samples could be extracted, handled and measured. Since some of the irradiations were planned with cadmium-covered foils and the prepared cadmium cups would require bigger holes, in total two aluminium sample holders were manufactured. One with smaller holes (7 mm in diameter and 1.2 mm deep) to hold the single foils and one with bigger holes to contain the cadmium cups with the foils inside (10 mm in diameter and 3 mm deep). The weight of a single sample holder was not quite 200 g.

The aluminium sample holder with the bigger slots can be seen in figure ???. The top of the sample holder is on the right. The points where the sample holder is pierced, were the

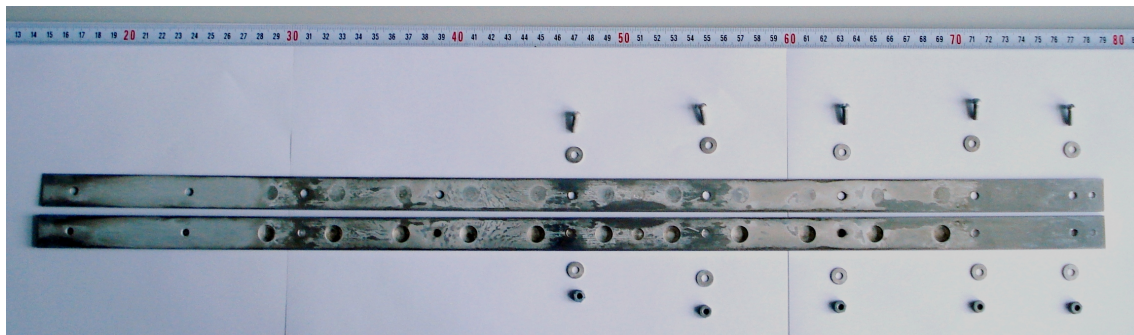


Figure 12.14: Aluminium sample holder used for irradiation of cadmium-covered foils in the central irradiation channel

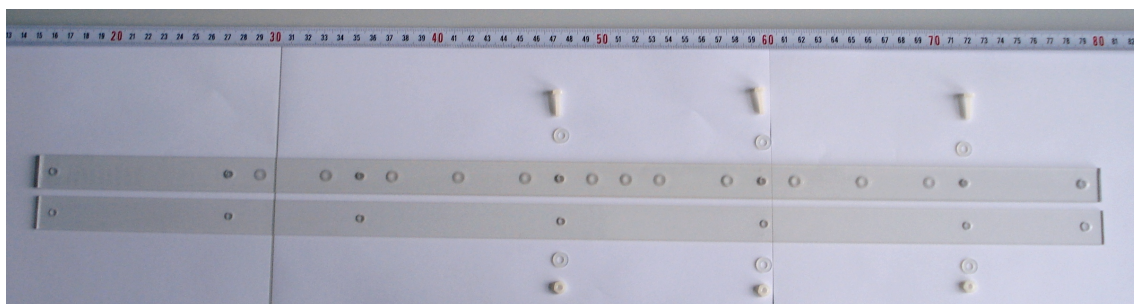


Figure 12.15: Sample holder made of MAKROLON[®] used for irradiation of aluminium foils in the central irradiation channel

positions of the aluminium screws as indicated for the top five screw positions. The sixth sample position –counted from either end– is the central position. The reference position can be seen right next to the central position. It is a little smaller than the other holes, since the reference foil did not have to be cadmium-covered.

Of course in the case of aluminium as an activation foil, the sample holder had to be made of some other material in order to be able to extract the sample holder quite shortly after irradiation and measure the desired reaction with the product of ^{27}Mg with its short half-life of approximately 9 min. Therefore, for the irradiations of aluminium there was an additional sample holder made of MAKROLON[®] by Bayer which is a polycarbonate. It had of course the exact same dimensions and sample positions as the sample holders made of aluminium. Only the number of screws was reduced which was mostly to quicken the extraction of the foils and be able to measure the foils a little earlier. This sample holder is displayed in figure ???. The equally spaced sample positions, as well as the reference position in between and the piercings for the plastic screws can be seen clearly.

Irradiations

The irradiations in the central irradiation channel were performed at a power of 1 kW with an irradiation time of usually 10 min but in the case of iron, nickel, and the cadmium-covered foils, namely gold and indium, it was increased to 30 min to achieve a better activation. In each irradiation a copper foil was placed in the reference position to act as a flux monitor.

All the general information concerning the irradiations in the central irradiation channel can be seen in table ???. The additional (Cd) next to the material denotes that these foils were covered with cadmium during irradiation. If there were two materials in an irradiation, the material that is listed first occupied the outer positions (Positions 1-3 and Positions 9-11, counted from the top of the sample holder), and the second material occupied the inner positions (Positions 4 - 8). The short half-life of ^{27}Mg from the activation of ^{27}Al lead to the necessity of performing two irradiations with aluminium, one for the top five positions and another one for the other 6 positions of the sample holder.

	Irradiated foils	Reference foil	Reactor power	Irradiation time
CT1	Fe	Cu	1 kW	30 min
CT2	Au + Cu	Cu	1 kW	10 min
CT3	Cu + Au	Cu	1 kW	11 min
CT4	Au(Cd) + In(Cd)	Cu	1 kW	30 min
CT5	Ni	Cu	1 kW	30 min
CT6	In(Cd) + Au(Cd)	Cu	1 kW	30 min
CT7	Al (Pos. 1-5)	Cu	1 kW	10 min
CT8	Al (Pos. 6-11)	Cu	1 kW	10 min

Table 12.4: Irradiations conducted in the central irradiation channel

12.4 Reactor Power Calibration

After evaluation of the first few irradiations it was noticed that the reference foils, that were placed in each irradiation to monitor the flux, exhibited strong fluctuations in their activities. After some investigation, this was ascribed to fluctuations of the reactor power level due to problems with the reactor instrumentation in particular the measuring channel NM-1000. The values that were reported by the two independent linear chambers NMP-Ph and NMP-Ch were considered to be more reliable.

Since this meant that the power level displayed by the instrumentation was not necessarily the actual power level, the use of reference foils as flux monitors proved redemptive. In the following irradiations, the values of the linear chambers were noted and kept at a more or less constant value.

At first it was assumed that the irradiations were performed at 1 kW since that was the power level displayed by the NM-1000. After noticing the problem with the display of the NM-1000, the power was kept the same for the following irradiations by considering the values of the linear chambers. The problem that occurred now, was that the exact power at which the irradiations had been performed was not known. To solve this question, a power calibration was performed.

The power calibration is based on the thermal heating of the pool water. If the power is exactly 100 kW the tank temperature increases by 5.19°C in one hour. If the temperature increase is higher than 5.19°C, the power heating the water must be more than 100 kW. This was determined experimentally through the insertion of five electrical heaters (with a mutual electrical power of 100 kW) into the core to heat up the pool water. The equation which describes this process is the following:

$$P \text{ [kW]} = \frac{\Delta T(1h) \text{ [}^\circ\text{C]}}{5.19^\circ\text{C}} \cdot 100 \quad (12.1)$$

To find out the actual reactor power, the reactor was kept at 100 kW and the increase of the pool temperature was monitored and noted for approximately 100 min. Afterwards, the pool temperature was plotted over time. A linear fit gave the exact temperature increase which was 4.7°C in this case. Thus, the actual reactor power was lower than 100 kW, namely 91.65 kW. The measuring chambers were then adjusted to show the correct values if they had not before.

After performing the power calibration the problem of the unknown power in the irradiations could be addressed: It is evident, that there should be a linear correlation between the saturated activity of a foil and the reactor power which was used to activate that particular foil. To find out what the exact reactor power in the previous irradiations had been, two more copper foils were irradiated in the reference position. One for 10 min at 5 kW and the other for 10 min at 250 kW. They were measured and extrapolated to saturation and then compared to one of the reference foils from the previous irradiations, namely the one from the CT6 irradiation.

Figure ?? shows the plot of the saturated activity over reactor power. The linear fit and its equation were used to determine the unidentified power level which was used for the activation of the reference foil in the CT6 irradiation. As will be discussed in the results, the activity values were normalized and scaled to one of the reference foils which was this particular reference foil in CT6.

The previously unknown power level was identified to be 1.2 kW.

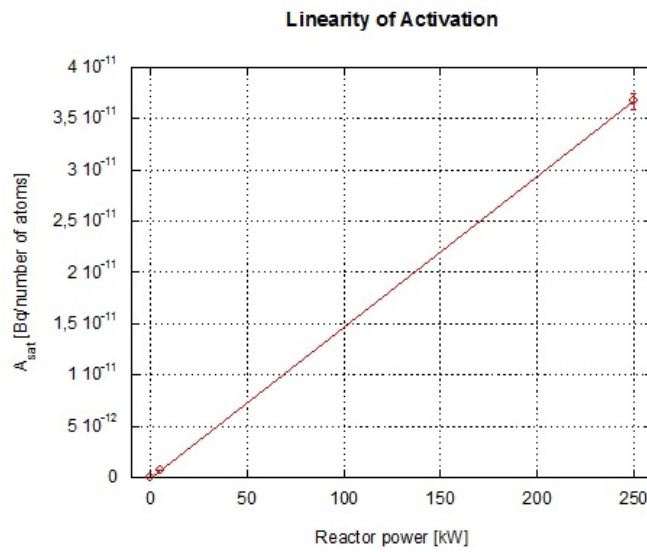


Figure 12.16: Saturated activity as a function of the reactor power level to illustrate the linearity of activation

Part III

Data Analysis and Conclusion

13 Data Analysis and Results

13.1 Calculations

Before presenting the results of the irradiations in both irradiation facilities, the horizontal beam tube and the central irradiation channel, the calculations that lead to these results will be discussed briefly. All the activities that are given are extrapolated to saturation and divided by the number of atoms in order to normalize the value with respect to the variations of the foil masses.

Detailed information about the concept of saturated activity can be found in section ?? . As a reminder, the saturated activity is calculated using the following equation:

$$A_{sat} = \frac{A_0}{(1 - e^{-\lambda t_i})} = A(t_d) \frac{e^{-\lambda t_d}}{(1 - e^{-\lambda t_i})} \quad (13.1)$$

where A_0 is the activity directly after irradiation, t_i is the irradiation time, t_d the cooling down period after irradiation, and λ is the decay constant. [?, p.1] [?, p.27ff]

$A(t_d)$ is the activity after cooling down. In this particular case it was also the measured activity since the software of the gamma detector which was used in the course of this work reported all the activities to the beginning of the measurement. Otherwise the decay during the counting time would have had to be included in the calculations, especially for nuclides with short half-lives such as ^{27}Mg .

It had to be taken into account, that the foils of the same material varied slightly in weight and therefore in the number of atoms. This was corrected by dividing the calculated saturated activity of a foil by its particular number of atoms. It is important to note, that the number of atoms refers to the atoms of the isotope of interest and not to all the atoms of the foil material. The following eq. ?? shows how the number of atoms was calculated using the measured weight of the foil, the pureness of the material as stated by the manufacturer, the atomic mass and the isotopic abundance.

$$N = \frac{m \cdot \text{pureness} \cdot \text{isotopic abundance} \cdot N_A}{\text{atomic mass}} \quad (13.2)$$

where N denotes the number of atoms of a certain isotope in a foil with mass, m , and N_A is

the Avogadro constant ($N_A = 6.022\,141\,29 \cdot 10^{23} \text{ mol}^{-1}$ [?]).

The constants and values that were used in the calculations can be seen in table ?? . The mass that is given, is a calculated value based on the geometry of the foils. The number of atoms is also a calculated value based on this mass. All the foils were weighted before irradiation and the calculations were performed using the exact mass of the particular foil and not these calculated values from the table. The pureness of the foil was provided by the manufacturer and can be found in the certificates in the appendix. The values for the isotopic abundance were taken from [?].

In table ?? the reactions of interest, the half-lives of the activation products and their respective decay constant, λ , can be seen.

Foil	Mass [mg]	Atomic mass [uma]	Pureness [%]	Isotope	Isotopic abundance	Number of atoms
Au	13.66	196.9666	99.99	Au-197	1	$4.176 \cdot 10^{19}$
Cu	126.58	62.9296	99.99	Cu-63	0.6915	$8.296 \cdot 10^{20}$
In	103.34	114.9039	99.999	In-115	0.9571	$5.187 \cdot 10^{20}$
Ni	125.85	57.9353	99.999	Ni-58	0.6808	$8.787 \cdot 10^{20}$
Fe	222.63	53.9369	99.99	Fe-54	0.0585	$1.404 \cdot 10^{20}$
Al	19.09	26.9815	99.999	Al-27	1	$4.261 \cdot 10^{20}$

Table 13.1: Important constants concerning activation foils

Foil	Reaction	Half-live	Decay constant λ [s^{-1}]
Au	$^{197}\text{Au}(n,\gamma)^{198}\text{Au}$	2.7 d	$2.976 \cdot 10^{-6}$
Cu	$^{63}\text{Cu}(n,\gamma)^{64}\text{Cu}$	12.7 h	$1.516 \cdot 10^{-5}$
In	$^{115}\text{In}(n,n')^{115}\text{In}^*$	4.36 h	$4.292 \cdot 10^{-5}$
Ni	$^{58}\text{Ni}(n,p)^{58}\text{Co}$	70.78 d	$1.133 \cdot 10^{-7}$
Fe	$^{54}\text{Fe}(n,p)^{54}\text{Mn}$	312.7 d	$2.567 \cdot 10^{-8}$
Al	$^{27}\text{Al}(n,p)^{27}\text{Mg}$	9.43 min	$1.220 \cdot 10^{-3}$

Table 13.2: Reactions, half-lives and decay constants for calculations

The activity values of the bare and cadmium-covered gold foils were corrected for self-shielding effects according to Westcott theory, see [?]. [?] [?]

13.2 Beam Tube - Results

In the following table ?? the saturated activities in [Bq/number of atoms] for the various foils in all three irradiation positions can be found. In figure ?? the decrease of the saturated activities of bare and cadmium-covered gold and copper foils along the beam tube, are illustrated. As expected, due to the decreasing neutron flux, the activation of the foils shows a noticeable decrease along the horizontal axis of the beam tube.

In table ?? and also in figure ?? it can be seen how the saturated activity of the foils corresponds to the reactions that had to be detected. Especially for the threshold reactions the activation is much lower which is due to the neutron flux. Reactions that can be initiated by all the neutrons in a reactor such as the (n,γ) reaction of ^{197}Au yield activation products with much higher activity than reactions that need particularly high neutron energies to take place such as for example the (n,p) reaction of ^{27}Al .

Statistical errors of the gamma spectroscopy measurements originated from the variation and optimisation of the cooling down period after irradiation and the counting time. In general, these uncertainties were less than 3% and varied for the particular foils. In respect to the systematic error of the measurement process, an activated gold foil was measured repeatedly. After each measurement it was taken out and placed again inside the detector before the next measurement with the same counting time was started. The error for this procedure was evaluated to be less than 2%. Thus the total uncertainty of the gamma spectroscopy measurements for the beam tube irradiations could be evaluated to be in the range of $\pm 5\%$. [?]

The further use of this data included neutron flux and neutron spectrum calculations. Preliminary data was published here [?].

Foil	Saturated activity [Bq/number of atoms]		
	Position 1 (5 cm from reflector)	Position 2 (125 cm from reflector)	Position 3 (185 cm from reflector)
Au	$(6.14 \pm 0.30) \cdot 10^{-11}$	$(2.70 \pm 0.13) \cdot 10^{-13}$	$(8.43 \pm 0.42) \cdot 10^{-14}$
Au(Cd)	$(4.52 \pm 0.23) \cdot 10^{-11}$	$(1.68 \pm 0.08) \cdot 10^{-13}$	$(5.78 \pm 0.29) \cdot 10^{-14}$
Cu	$(1.22 \pm 0.06) \cdot 10^{-12}$	$(5.04 \pm 0.25) \cdot 10^{-15}$	$(1.18 \pm 0.06) \cdot 10^{-15}$
In(Cd)	$(8.09 \pm 0.40) \cdot 10^{-15}$	$(1.98 \pm 0.10) \cdot 10^{-16}$	not irradiated
Ni	$(6.20 \pm 0.31) \cdot 10^{-15}$	$(1.67 \pm 0.08) \cdot 10^{-16}$	not irradiated
Fe	$(3.34 \pm 0.17) \cdot 10^{-15}$	not measurable	not irradiated
Al	$(2.06 \pm 0.10) \cdot 10^{-16}$	$(6.11 \pm 0.30) \cdot 10^{-18}$	not irradiated

Table 13.3: Saturated activities for the irradiations in the beam tube positions

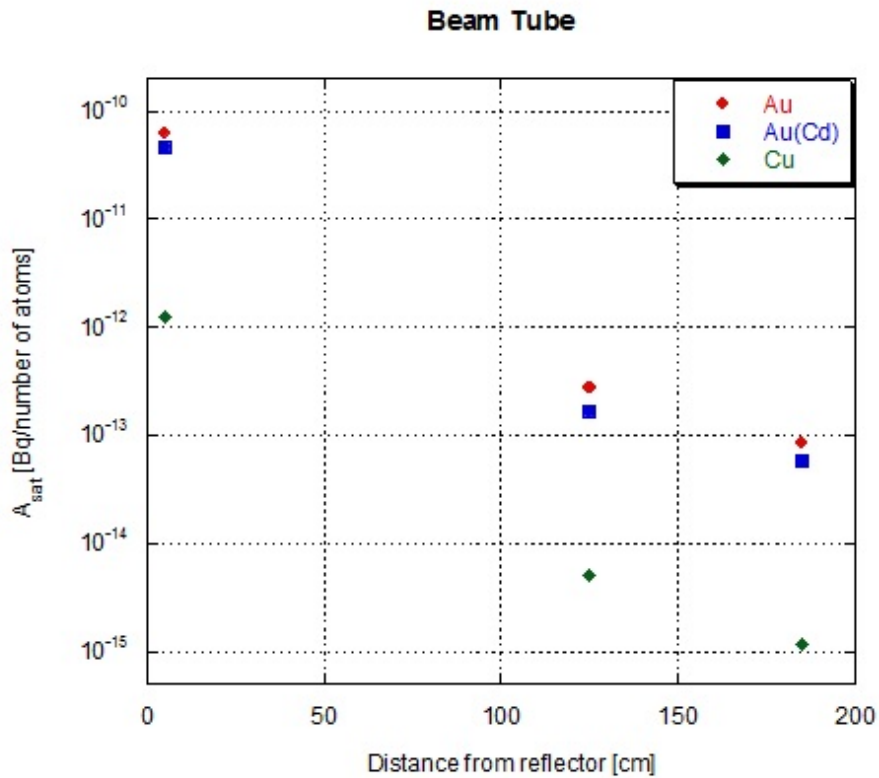


Figure 13.1: Saturated activities of gold, cadmium-covered gold and copper foils as a function of the distance from the reflector

13.3 Central Irradiation Channel - Results

As mentioned earlier, copper reference foils were placed as a means of monitoring the neutron flux and power level in all the irradiations in the central irradiation channel. This was necessary because the irradiations were performed at different times and under slightly different circumstances.

The following table ?? contains the saturated activities for the reference foils for each irradiation performed in the central irradiation channel. To normalize the data, all the activities were reported to one irradiation, in particular CT6. In this way, the correction factor which was used to scale all the calculated activities in the respective irradiations was calculated. This correction factor can also be found in table ??.

	A_{sat} [Bq/number of atoms]	Correction factor
CT1	$(1.23 \pm 0.04) \cdot 10^{-13}$	0.699
CT2	$(1.12 \pm 0.03) \cdot 10^{-13}$	0.636
CT3	$(1.73 \pm 0.05) \cdot 10^{-13}$	0.983
CT4	$(1.63 \pm 0.05) \cdot 10^{-13}$	0.926
CT5	$(1.88 \pm 0.05) \cdot 10^{-13}$	1.068
CT6	$(1.76 \pm 0.05) \cdot 10^{-13}$	1.000
CT7	$(2.12 \pm 0.06) \cdot 10^{-13}$	1.205
CT8	$(2.06 \pm 0.06) \cdot 10^{-13}$	1.170

Table 13.4: Evaluation of the reference foils: saturated activities, A_{sat} , in [Bq/number of atoms] for the reference foils and the calculated correction factor used to normalize the activities

In the following tables ?? – ?? the results for the various irradiations can be found. It is important to note, that these activity values have been normalized by scaling them to the CT6 irradiation. It was deemed best to present the data for each foil material instead of the single irradiations. The tables include the foil position in the sample holder, the distance from the central position –which should be equivalent to the centre of the reactor core– and the normalized saturated activity values.

Additionally, the obtained data was plotted for all the foils and can be found below the tables in figures ?? – ?. It can be seen very well that the saturated activity reaches its maximum in the central position and that the foils which are positioned on the top or bottom of the sample holder show the smallest activity values because of reduced activation due to decreased neutron flux.

Results for Au		
	Distance from centre [cm]	A_{sat} [Bq/number of atoms]
Position 1	20	$(3.26 \pm 0.07) \cdot 10^{-12}$
Position 2	16	$(4.61 \pm 0.10) \cdot 10^{-12}$
Position 3	12	$(5.87 \pm 0.13) \cdot 10^{-12}$
Position 4	8	$(6.57 \pm 0.14) \cdot 10^{-12}$
Position 5	4	$(7.22 \pm 0.16) \cdot 10^{-12}$
Position 6	0	$(7.44 \pm 0.16) \cdot 10^{-12}$
Position 7	-4	$(7.22 \pm 0.16) \cdot 10^{-12}$
Position 8	-8	$(6.40 \pm 0.14) \cdot 10^{-12}$
Position 9	-12	$(5.39 \pm 0.12) \cdot 10^{-12}$
Position 10	-16	$(3.84 \pm 0.08) \cdot 10^{-12}$
Position 11	-20	$(2.62 \pm 0.06) \cdot 10^{-12}$

Table 13.5: Central irradiation channel: results for gold foils

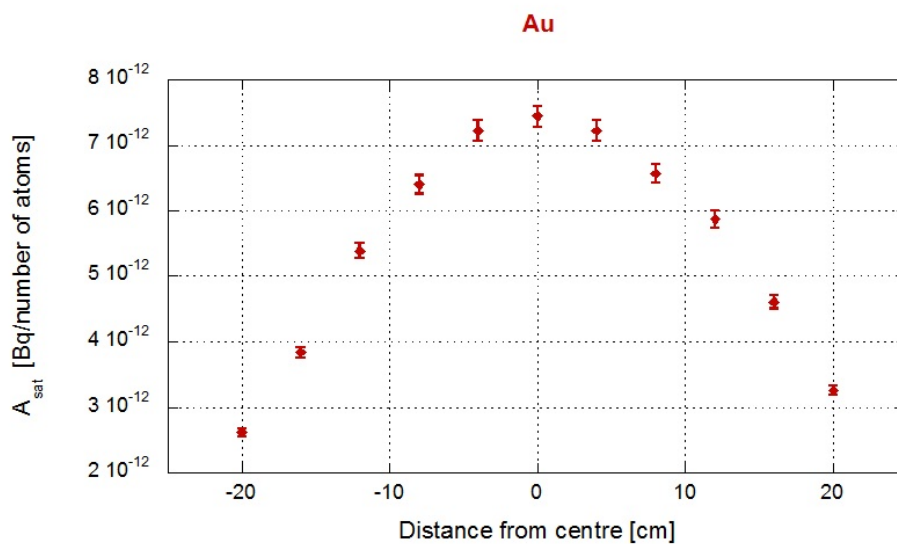


Figure 13.2: Saturated activity of the gold foils plotted over distance from the centre of the reactor core

Results for Au(Cd)		
	Distance from centre [cm]	A_{sat} [Bq/number of atoms]
Position 1	20	$(1.98 \pm 0.04) \cdot 10^{-12}$
Position 2	16	$(2.62 \pm 0.06) \cdot 10^{-12}$
Position 3	12	$(3.26 \pm 0.07) \cdot 10^{-12}$
Position 4	8	$(2.94 \pm 0.06) \cdot 10^{-12}$
Position 5	4	$(3.15 \pm 0.07) \cdot 10^{-12}$
Position 6	0	$(3.30 \pm 0.07) \cdot 10^{-12}$
Position 7	-4	$(3.19 \pm 0.07) \cdot 10^{-12}$
Position 8	-8	$(2.87 \pm 0.07) \cdot 10^{-12}$
Position 9	-12	$(2.85 \pm 0.06) \cdot 10^{-12}$
Position 10	-16	$(1.95 \pm 0.04) \cdot 10^{-12}$
Position 11	-20	$(1.24 \pm 0.03) \cdot 10^{-12}$

Table 13.6: Central irradiation channel: results for cadmium-covered gold foils

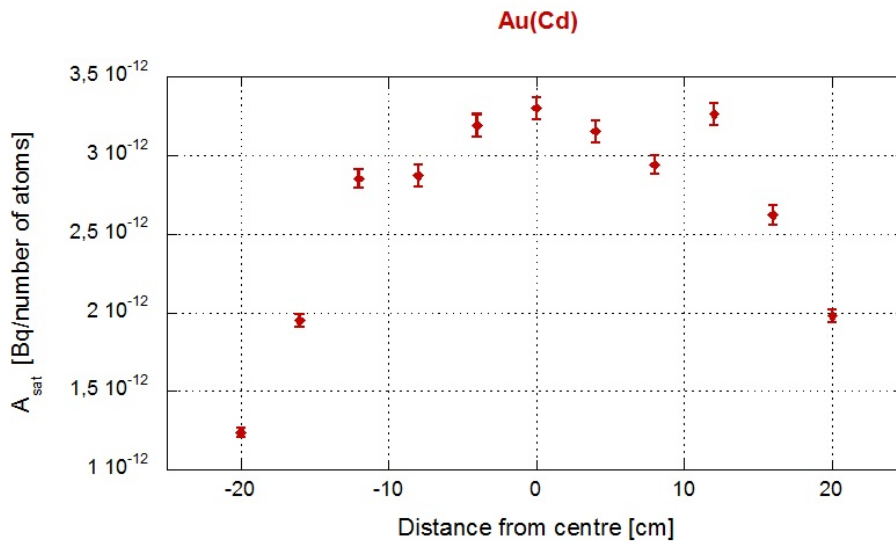


Figure 13.3: Saturated activity of the cadmium-covered gold foils plotted over distance from the centre of the reactor core

Results for Cu		
	Distance from centre [cm]	A_{sat} [Bq/number of atoms]
Position 1	20	$(7.49 \pm 0.22) \cdot 10^{-14}$
Position 2	16	$(1.06 \pm 0.03) \cdot 10^{-13}$
Position 3	12	$(1.34 \pm 0.04) \cdot 10^{-13}$
Position 4	8	$(1.53 \pm 0.06) \cdot 10^{-13}$
Position 5	4	$(1.66 \pm 0.06) \cdot 10^{-13}$
Position 6	0	$(1.68 \pm 0.05) \cdot 10^{-13}$
Position 7	-4	$(1.65 \pm 0.07) \cdot 10^{-13}$
Position 8	-8	$(1.52 \pm 0.06) \cdot 10^{-13}$
Position 9	-12	$(1.24 \pm 0.03) \cdot 10^{-13}$
Position 10	-16	$(8.85 \pm 0.27) \cdot 10^{-14}$
Position 11	-20	$(6.40 \pm 0.19) \cdot 10^{-14}$

Table 13.7: Central irradiation channel: results for copper foils

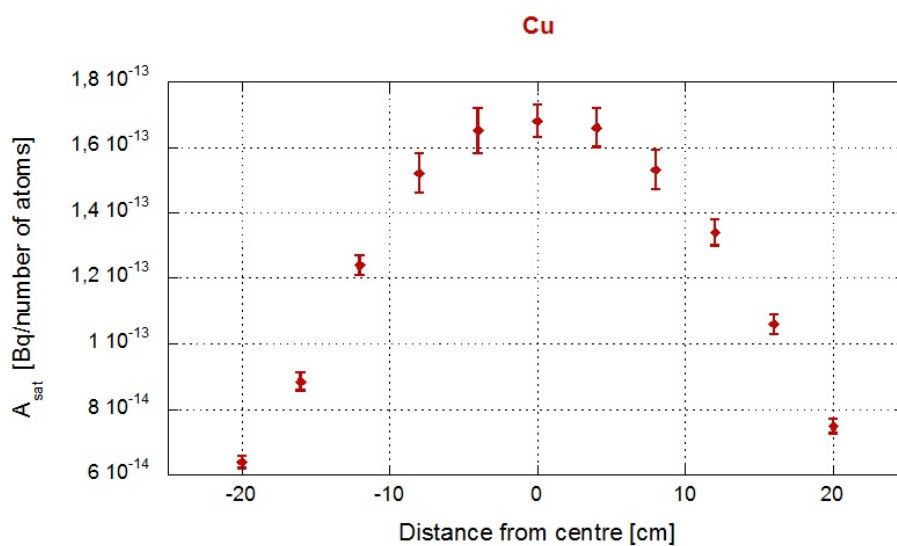


Figure 13.4: Saturated activity of the copper foils plotted over distance from the centre of the reactor core

Results for In(Cd)		
	Distance from centre [cm]	A_{sat} [Bq/number of atoms]
Position 1	20	$(1.71 \pm 0.04) \cdot 10^{-15}$
Position 2	16	$(2.76 \pm 0.06) \cdot 10^{-15}$
Position 3	12	$(3.54 \pm 0.08) \cdot 10^{-15}$
Position 4	8	$(4.16 \pm 0.10) \cdot 10^{-15}$
Position 5	4	$(4.50 \pm 0.11) \cdot 10^{-15}$
Position 6	0	$(4.67 \pm 0.12) \cdot 10^{-15}$
Position 7	-4	$(4.42 \pm 0.11) \cdot 10^{-15}$
Position 8	-8	$(3.92 \pm 0.09) \cdot 10^{-15}$
Position 9	-12	$(3.13 \pm 0.08) \cdot 10^{-15}$
Position 10	-16	$(1.99 \pm 0.05) \cdot 10^{-15}$
Position 11	-20	$(9.54 \pm 0.22) \cdot 10^{-16}$

Table 13.8: Central irradiation channel: results for cadmium-covered indium foils

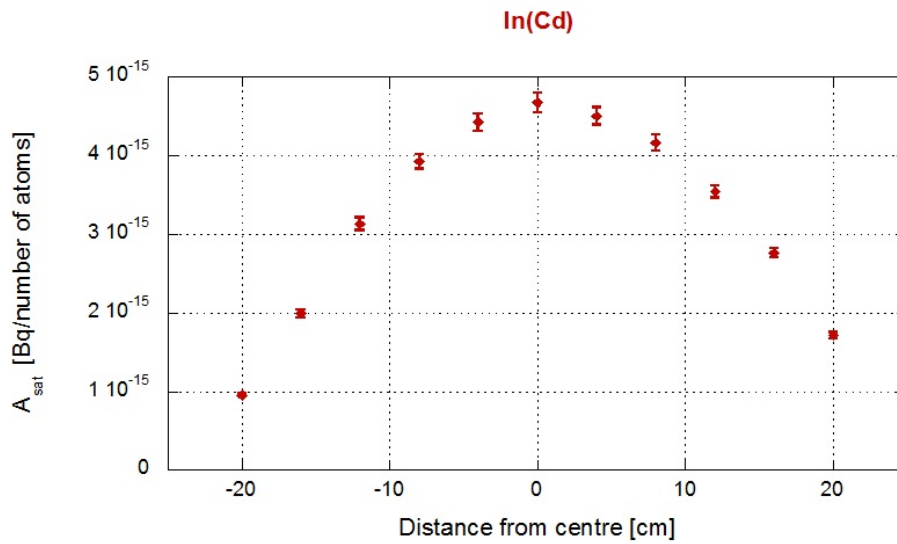


Figure 13.5: Saturated activity of the cadmium-covered indium foils plotted over distance from the centre of the reactor core

Results for Ni		
	Distance from centre [cm]	A_{sat} [Bq/number of atoms]
Position 1	20	$(8.87 \pm 0.20) \cdot 10^{-16}$
Position 2	16	$(1.34 \pm 0.03) \cdot 10^{-15}$
Position 3	12	$(1.71 \pm 0.04) \cdot 10^{-15}$
Position 4	8	$(1.97 \pm 0.05) \cdot 10^{-15}$
Position 5	4	$(2.18 \pm 0.05) \cdot 10^{-15}$
Position 6	0	$(2.21 \pm 0.05) \cdot 10^{-15}$
Position 7	-4	$(2.11 \pm 0.05) \cdot 10^{-15}$
Position 8	-8	$(1.86 \pm 0.04) \cdot 10^{-15}$
Position 9	-12	$(1.46 \pm 0.04) \cdot 10^{-15}$
Position 10	-16	$(8.93 \pm 0.20) \cdot 10^{-16}$
Position 11	-20	$(4.21 \pm 0.09) \cdot 10^{-16}$

Table 13.9: Central irradiation channel: results for nickel foils

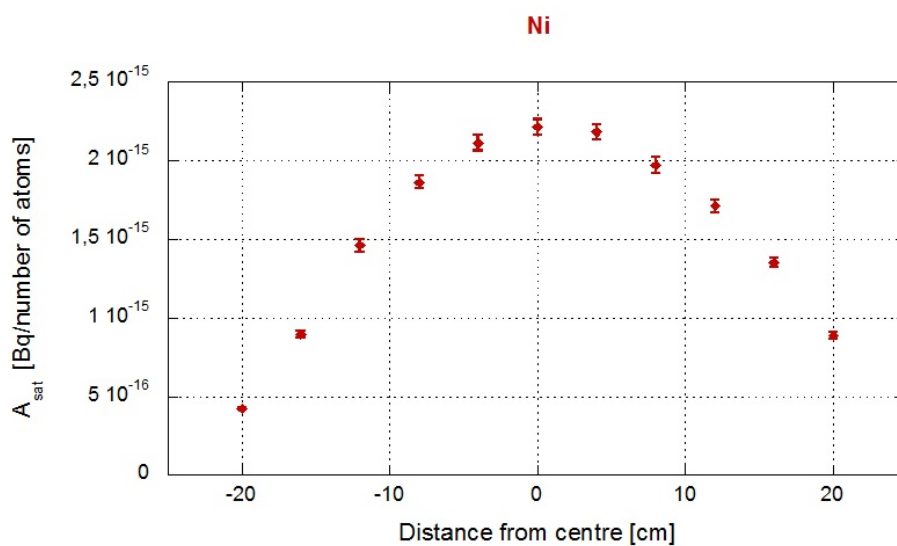


Figure 13.6: Saturated activity of the nickel foils plotted over distance from the centre of the reactor core

Results for Fe		
	Distance from centre [cm]	A_{sat} [Bq/number of atoms]
Position 1	20	$(6.25 \pm 0.19) \cdot 10^{-16}$
Position 2	16	$(9.57 \pm 0.28) \cdot 10^{-16}$
Position 3	12	$(1.23 \pm 0.04) \cdot 10^{-15}$
Position 4	8	$(1.40 \pm 0.05) \cdot 10^{-15}$
Position 5	4	$(1.61 \pm 0.05) \cdot 10^{-15}$
Position 6	0	$(1.59 \pm 0.05) \cdot 10^{-15}$
Position 7	-4	$(1.51 \pm 0.05) \cdot 10^{-15}$
Position 8	-8	$(1.33 \pm 0.04) \cdot 10^{-15}$
Position 9	-12	$(1.06 \pm 0.03) \cdot 10^{-15}$
Position 10	-16	$(6.48 \pm 0.25) \cdot 10^{-16}$
Position 11	-20	$(3.10 \pm 0.12) \cdot 10^{-16}$

Table 13.10: Central irradiation channel: results for iron foils

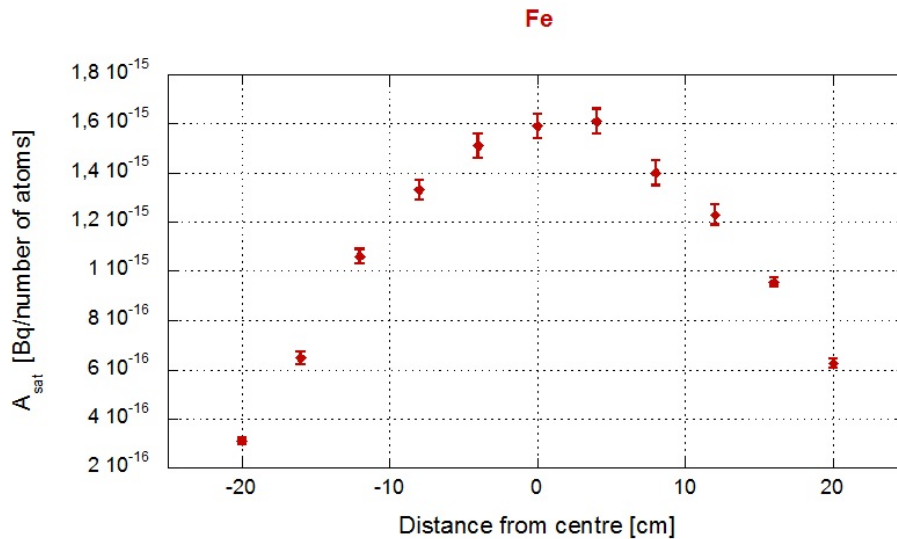


Figure 13.7: Saturated activity of the iron foils plotted over distance from the centre of the reactor core

Results for Al		
	Distance from centre [cm]	A_{sat} [Bq/number of atoms]
Position 1	20	$(2.99 \pm 0.14) \cdot 10^{-17}$
Position 2	16	$(4.50 \pm 0.21) \cdot 10^{-17}$
Position 3	12	$(6.16 \pm 0.31) \cdot 10^{-17}$
Position 4	8	$(7.07 \pm 0.38) \cdot 10^{-17}$
Position 5	4	$(8.28 \pm 0.51) \cdot 10^{-17}$
Position 6	0	$(8.48 \pm 0.30) \cdot 10^{-17}$
Position 7	-4	$(8.06 \pm 0.29) \cdot 10^{-17}$
Position 8	-8	$(7.17 \pm 0.26) \cdot 10^{-17}$
Position 9	-12	$(5.87 \pm 0.21) \cdot 10^{-17}$
Position 10	-16	$(3.64 \pm 0.17) \cdot 10^{-17}$
Position 11	-20	$(1.64 \pm 0.07) \cdot 10^{-17}$

Table 13.11: Central irradiation channel: results for aluminium foils

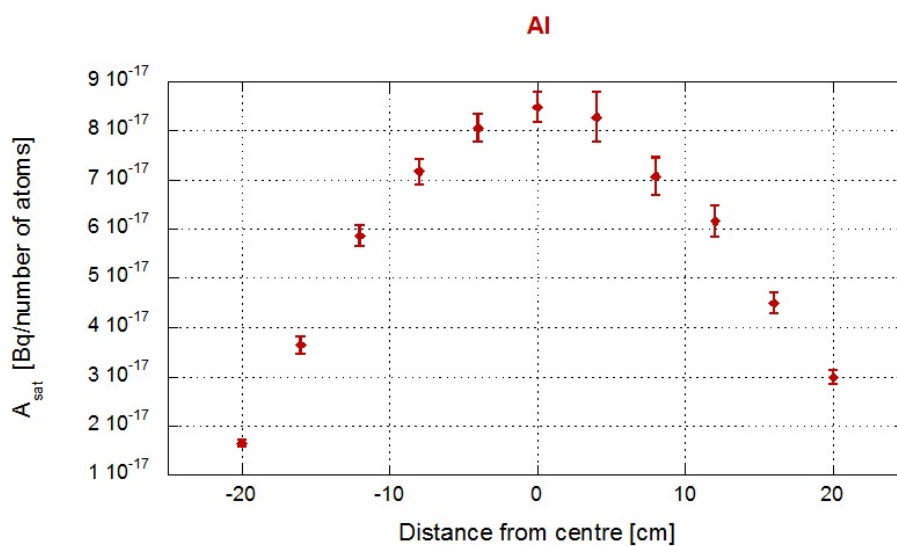


Figure 13.8: Saturated activity of the aluminium foils plotted over distance from the centre of the reactor core

The statistical error for all the gamma spectroscopy measurements was in the range of 0.2% – 3%, depending on the particular foil. The systematic error was investigated by measuring the same activated gold foil repeatedly, always taking it out and replacing it on the detector. The uncertainty for this process was less than 2%. The total uncertainty of the gamma spectroscopy measurements was therefore in the range of 2.2 – 5%. [?]

Preliminary data of the further use of the measurements is published here [?].

14 Conclusion

The measurements, which were performed in the course of this master thesis, were used for an ongoing research project at the Atominstitut related to the neutron flux characterization of the new core. Thus it was of the utmost importance to reduce uncertainties to minimize the propagation of errors. This was achieved by optimizing the irradiation, cooling down and measurement process.

The sample holders were made of different materials in order to meet the specific needs of the activation foils. They were designed to achieve the best activation of the foils without influencing the neutron flux itself. Furthermore, they had to be thin and light in the interest of minimising the material and thus the sample holder activity. This was done in pursuance of a reduction of the cooling down time in the reactor tank. Additionally, to reduce the time spent working close to the radioactive materials, the sample holders had to be easy to handle and open.

The irradiation time had to be long enough to activate the foils sufficiently, to be able to detect the desired reaction, but was restricted due to reactor availability and of course the activation of the sample holder. For the same reasons the power used was limited. A higher power level would have meant a stronger activation but also a longer cooling down period before the foils could have been handled. That would not have been possible in the case of the short-lived radionuclides such as ^{27}Mg , $^{115}\text{In}^*$ and ^{64}Cu . They would have decayed before the sample holder could have been taken out of the reactor safely according to radiation protection considerations.

The measurement process was defined mostly by the counting time. Usually, the longer the counting time, the smaller is the error of a measurement. But sometimes the counting time is limited by the growth of daughter nuclides with gamma energy peaks close to the nuclide of interest in the sample. This was the case for ^{27}Mg , where a gamma peak of ^{54}Mn due to a small iron impurity would have overlapped with the ^{27}Mg peak. In order to avoid this double peak the counting time was limited. On the other hand, the high dead time of the detector sometimes called for longer cooling down periods before measurement to allow the decay of other gamma energy peaks that were not of interest. This was the case for $^{115}\text{In}^*$ as well as for ^{64}Cu .

Altogether, the occurring challenges were handled very effectively by optimising the irradi-

14 Conclusion

ation process as well as the cooling down and counting time with regard to the particular activation foil. The uncertainties of the measurements were in a thoroughly satisfying range, lower than 5%.

15 Bibliography

- [1] W. Stolz. *Radioaktivität: Grundlagen - Messung - Anwendung (5. überarbeitete und erweiterte Auflage)*. B.G. Teubner-Verlag, Wiesbaden, 2005.
- [2] B. Bröcker. *dtv-Atlas zur Atomphysik - Tafeln und Texte (5. Auflage)*. Deutscher Taschenbuch Verlag, München, 1993.
- [3] M.F. L'Annunziata. *Handbook of Radioactivity Analysis (Third edition)*. Academic Press (Elsevier Inc.), Oxford, Amsterdam, Waltham, San Diego, 2012.
- [4] J. Magill G. Pfennig R. Dreher Z. Sóti. *Karlsruher Nuklidkarte (8. Auflage)*. Nucleonica GmbH, Karlsruhe, 2012.
- [5] J.R. Lamarsh. *Introduction to Nuclear Reactor Theory*. Addison-Wesley Publishing Company, 1972.
- [6] T. Mayer-Kuckuk. *Kernphysik - Eine Einführung (7. überarbeitete und erweiterte Auflage)*. B.G. Teubner, Stuttgart, Leipzig, Wiesbaden, 2002.
- [7] Commonwealth Scientific and Industrial Research Organisation (CSIRO) Australia Telescope National Facility. Alpha decay. www.atnf.csiro.au/outreach//education/senior/cosmicengine/images/sun/alphadecay.gif (access date: 26 February, 2015).
- [8] M. Bichler. *Aktivierungsanalyse - Grundlagen und Anwendungen*, 1996. Vorlesungsskriptum.
- [9] M. Villa. *Reaktorphysik*, 2008. Vorlesungsskriptum, AIAU 98402.
- [10] National Nuclear Data Center. *Experimental Nuclear Reaction Data (EXFOR)*. <http://www.nndc.bnl.gov/exfor/exfor.htm> (access date: 14 April, 2014).
- [11] Jr. W.S. Lyon. *Guide to Activation Analysis*. D. Van Nostrand Company, Inc., Princeton, New Jersey, 1964.
- [12] W.R. Leo. *Techniques for Nuclear and Particle Physics Experiments*. Springer-Verlag, Berlin, Heidelberg, New York, 1987.

- [13] ICRP. *Annals of the ICRP: ICRP Publication 103 - The 2007 Recommendations of the International Commission on Radiological Protection*. Elsevier Ltd., 2007.
- [14] ICRP. *Annals of the ICRP: ICRP Publication 60 - 1990 Recommendations of the International Commission on Radiological Protection*. Pergamon Press, 1991.
- [15] R.H. Filby. *Isotopic and Nuclear Analytical Techniques in Biological Systems: A Critical Study - Part IX. Neutron Activation Analysis (Technical Report)*. *Pure & Appl. Chem.*, Vol.67, Co. 11:pp1929–1941, 1995.
- [16] IAEA. *Use of Research Reactors for Neutron Activation Analysis* (IAEA-TECDOC-1215), IAEA, Vienna, 2001.
- [17] H. Böck. *Neutron Activation Foil Manual*, 1989. AIAU 89306.
- [18] C.M. Fleck F. Bensch. *Neutronenphysikalisches Praktikum I (B.I. Hochschultaschenbücher 170/170a)*. Bibliographisches Institut AG, Mannheim, Deutschland, 1968.
- [19] K. Wirtz K.H. Beckurts. *Neutron Physics*. Springer-Verlag, Berlin, Göttingen, Heidelberg, New York, 1964.
- [20] M. Villa H. Böck. *Praktische Übungen am Reaktor*, 2005. Vorlesungsskriptum, AIAU 25315.
- [21] R. Khan. *Neutronics Analysis of the TRIGA Mark II Research Reactor and its Experimental Facilities*, 2010. PhD dissertation, Vienna University of Technology, Vienna.
- [22] General Atomic (GA). *TRIGA Mark II Reactor General Specifications and Description*. General Atomic Company, USA, March 1964.
- [23] M. Cagnazzo C.Raith M. Villa H. Böck. *Measurements of the in-core neutron flux distribution and energy spectrum at the TRIGA Mark II reactor of the Vienna University of Technology/Atomintitut*, 2014. No. 702 in Proceedings of 23rd International Conference Nuclear Energy for New Europe NENE 2014, Portorož, Slovenia, September 8-11. ISBN: 978-961-6207-37-9.
- [24] Canberra Industries Inc. *Genie™ 2000 Spectroscopy Software - Operations Manual (v. 3.1)*. Canberra Industries Inc., Meriden, 2006.
- [25] Canberra Industries Inc. *Genie™ 2000 Spectroscopy Software - Customizations Tools Manual (v. 3.1)*. Canberra Industries Inc., Meriden, 2006.
- [26] Canberra Industries Inc. *Genie™ 2000 Tutorials*. Canberra Industries Inc., Meriden, 2004.

- [27] National Nuclear Data Center. *Chart of Nuclides database*. www.nndc.bnl.gov/chart/ (access date: 14 April, 2014).
- [28] M. Cagnazzo C.Raith T. Stummer M. Villa H. Böck. *Measurements of neutron flux distribution and energy spectrum in the horizontal beam tube at the TRIGA Mark II reactor Vienna*. RRFM Transactions 2014, European Nuclear Society, Brüssel, 2014. ISBN: 978-92-95064-20-1, 336 - 342.
- [29] The NIST Reference on Constants, Units and Uncertainty. www.physics.nist.gov/cgi-bin/cuu/Value?na (access date: 24 April, 2015).
- [30] CIAAW - Commission on Isotopic Abundances and Atomic Weights. www.ciaaw.org (access date: 24 April, 2015).
- [31] T.K. Alexander C.H. Westcott, W.H. Walter. *Effective cross sections and cadmium ratios for the neutron spectra of thermal reactors*. A/CONF.15/P/202 Canada 26 May 1958, 1958.

Part IV

Appendix

A Detector Data Sheet

Following the 'detector specification and performance data' sheet for the gamma detector, which was used to perform gamma spectroscopy measurements.



DETECTOR SPECIFICATION AND PERFORMANCE DATA

Specifications

Detector Model GC5020 Serial number b 07133
 Cryostat Model 7500SL-RDC-4-ULB
 Preamplifier Model 2002CSL

The purchase specifications and therefore the warranted performance of this detector are as follows :

Nominal volume cc Relative efficiency 50 %
 Resolution 2.0 keV (FWHM) at 1.33 MeV
 keV (FWTM) at 1.33 MeV
 1.10 keV (FWHM) at 122 keV
 keV (FWTM) at
 Peak/Compton 62:1 Cryostat well diameter Well depth mm
 Cryostat description or Drawing Number if special Vertical dipstick, type 7500SL-RDC-4-ULB

Physical Characteristics

Geometry Coaxial one open end, closed end facing window
 Diameter 65 mm Active volume cc
 Length 68 mm Crystal well depth mm
 Distance from window (outside) 5 mm Crystal well diameter mm

Electrical Characteristics

Depletion voltage (+)3000 Vdc
 Recommended bias voltage Vdc (+)3500 Vdc
 Leakage current at recommended bias 0.01 nA
 Preamplifier test point voltage at recommended voltage -1.1 Vdc

Resolution and Efficiency

With amp time constant of 4 μ s

Isotope	⁵⁷ Co	⁶⁰ Co			
Energy (keV)	122	1332			
FWHM (keV)	.980	1.81			
FWTM (keV)		3.34			
Peak/Compton		73.6:1			
Rel. Efficiency		52.8%			

- Tests are performed following IEEE standard test ANSI/IEEE std325-1996
- Standard Canberra electronics used - See Germanium detector manual Section 7

Tested by : Date : April 26, 2007

Approved by : Date : April 26, 2007

B Calibration Source

In the following the calibration certificate for the reference source used for calibration of the gamma detector as provided by the manufacturer Eckert & Ziegler Nuclitec GmbH.

Eckert & Ziegler Nuclitec GmbH
Gieselweg 1
38110 Braunschweig
Tel +49 5307 932-0
Fax +49 5307 932-293

akkreditiert durch die / accredited by the

Deutsche Akkreditierungsstelle GmbH



Deutsche
Akkreditierungsstelle
D-K-15203-01-00

als Kalibrierlaboratorium im / as calibration laboratory in the

Deutschen Kalibrierdienst



Kalibrierschein
Calibration certificate

Kalibrierzeichen
Calibration mark

026560
D-K- 15203-01-00
2013-10

Strahler Nr. / Source number AD-1207

Gegenstand
Object **Gamma Referenzstrahler**

Hersteller
Manufacturer **Eckert & Ziegler Nuclitec GmbH**

Typ
Type **QCRB1186**

Strahler-Nr.
Source number **AD-1207**

Auftraggeber
Customer **Technische Universität Wien
1020 Wien
Österreich**

Auftragsnummer
Order No. **CO00157020**

Anzahl der Seiten des Kalibrierscheines
Number of pages of the certificate **2**

Dieser Kalibrierschein dokumentiert die Rückführung auf nationale Normale zur Darstellung der Einheiten in Übereinstimmung mit dem Internationalen Einheitensystem (SI).

Die DAkkS ist Unterzeichner der multilateralen Übereinkommen der European co-operation for Accreditation (EA) und der International Laboratory Accreditation Cooperation (ILAC) zur gegenseitigen Anerkennung der Kalibrierscheine.

Für die Einhaltung einer angemessenen Frist zur Wiederholung der Kalibrierung ist der Benutzer verantwortlich.

This calibration certificate documents the traceability to national standards, which realize the units of measurement according to the International System of Units (SI).

The DAkkS is signatory to the multilateral agreements of the European co-operation for Accreditation (EA) and of the International Laboratory Accreditation Cooperation (ILAC) for the mutual recognition of calibration certificates.

The user is obliged to have the object recalibrated at appropriate intervals.

Datum der Kalibrierung
Date of calibration **1. Oktober 2013**

Dieser Kalibrierschein darf nur vollständig und unverändert weiterverbreitet werden. Auszüge oder Änderungen bedürfen der Genehmigung sowohl der Deutschen Akkreditierungsstelle GmbH als auch des ausstellenden Kalibrierlaboratoriums. Kalibrierscheine ohne Unterschrift haben keine Gültigkeit.

This calibration certificate may not be reproduced other than in full except with the permission of both the Deutsche Akkreditierungsstelle GmbH and the issuing laboratory. Calibration certificates without signature are not valid.

Datum
Date

Leiter des Kalibrierlaboratoriums
Head of the calibration laboratory

Bearbeiter
Person in charge

30. Oktober 2013

Dr. Thieme

Schueler

Gamma-Referenzstrahler

Strahler-Nr. AD-1207
 Zeichnung VZ-1159-001
 Abmessungen der aktiven Oberfläche Ø 10 mm
 Gesamtabmessungen Ø 54 mm x 3 mm
 Strahleraufbau Das Radionuklidgemisch ist homogen auf der aktiven Fläche der Kunststoff-Folie verteilt. Die aktivierte Folie wird beidseitig jeweils durch ein Papierschild und eine Kunststoff-Folie abgedeckt.

Nuklid	Photonen-Energie [MeV]	Aktivität [Bq]	Photonen [s ⁻¹]
Americium-241	0,060	3,39E03	1,22E03
Cadmium-109	0,088	1,47E04	5,34E02
Cobalt-57	0,122	5,73E02	4,90E02
Cer-139	0,166	6,96E02	5,56E02
Quecksilber-203	0,279	1,42E03	1,16E03
Zinn-113	0,392	2,47E03	1,60E03
Strontium-85	0,514	2,80E03	2,76E03
Cäsium-137	0,662	2,77E03	2,36E03
Yttrium-88	0,898	5,17E03	4,86E03
Cobalt-60	1,173	3,21E03	3,20E03
Cobalt-60	1,333	3,21E03	3,21E03
Yttrium-88	1,836	5,17E03	5,14E03

Referenzdatum 1. Oktober 2013 um 12:00 UTC
 Dichtheits- und Kontaminationsprüfung Wischtest nach DIN 25426, Teil 3
 Wischtest bestanden am 30. Oktober 2013
 Messmethode Die Aktivität des Strahlers wurde durch Vergleich mit Referenzstrahlern gleichen Aufbaus bestimmt. Die Messung erfolgte an einem Reinstgermanium-Detektor mit Vielkanalanalysator.
 Messunsicherheit Die relative Messunsicherheit der Aktivität beträgt 3 % (Cd-109: 5 %).
 Angegeben ist die erweiterte Messunsicherheit, die sich aus der Standardmessunsicherheit durch Multiplikation mit dem Erweiterungsfaktor k = 2 ergibt. Sie wurde gemäß DAkkS-DKD-3 ermittelt. Der Wert der Messgröße liegt mit einer Wahrscheinlichkeit von 95 % im zugeordneten Wertebereich.
 Radioaktive Verunreinigungen Zum Zeitpunkt der Kalibrierung konnten folgende radioaktiven Verunreinigungen nachgewiesen werden:
 Rb-84 < 1 Bq; Ag-110m < 2 Bq; Cs-134 < 2 Bq
 Qualitätssicherungssystem Das Qualitätssicherungssystem von Eckert & Ziegler Nuclitec GmbH wurde durch Lloyds's Register Quality Assurance (LRQA) nach der ISO 9001 in der Ausgabe von 2008 zertifiziert.

C Foil Certificates

In the following the delivery sheet and the certificates of all the foils used in the various irradiations.

ADVICE NOTE



Ermine Business Park
 Huntingdon PE29 6WR England
 Telephone +44 1480 424 800
 Fax +44 1480 424 900

The goods shown on this advice note were despatched on the date and by the method shown.

Technische Universität Wien
 Stadionallee 2
 A-1020 WIEN
 AUSTRIA

For the attention of:
 Dr Mario Villa

Your order number 327

Date of your order 22-July-2013

Our order reference LS411293/S M B

Customer reference no. 12002-40

Invoice number 220249
 Order complete

Date of despatch 9-September-2013

5716 629 436 71
 2 9-September-2013

Item	Catalogue number	Material	Description		Condition of material	Quantity ordered	Quantity despatched	Harmonised tariff number
1	AU000341 390-826-75	Gold 99.99+ %*	Thickness 0.025mm	Diameter 6 mm	AR NLT	50 discs	None	71081380
2	CU000745 624-554-73	Copper 99.99+ %*	Thickness 0.5mm	Diameter 6 mm	AR LT	50 discs	None	74091900
3	NI000605 527-482-08	Nickel 99.999 %*	Thickness 0.5mm	Diameter 6 mm	AR LT	50 discs	50 discs	75061000
4	IN000266 839-500-27	Indium 99.999 %*	Thickness 0.5mm	Diameter 6 mm	AR LT	50 discs	None	81129970
5	AL000630 610-344-42	Aluminium 99.999 %*	Thickness 0.25mm	Diameter 6 mm	AR LT	50 discs	None	76061193
6	FE000411	Iron discs	Fe 99.99%			50 pcs	None Nil	
		Temper : As rolled						
		Thickness : 1.0mm +/-10%						
		Diameter : 6.0mm +/-0.5mm						

As all items have been ordered together, we have applied a discount of 5.0%

S M Burton 3-September-2013 : We will ship all material except item 3, this will follow as soon as possible.

Despatch to:

as shown above

Parcel type
1 Polythene Transit Bag

Net weight
6.29 g

Gross weight
134 g

Size
17 x 17 x 1.5 cm

Contents
1 Package

Method of despatch
FedEx Air Express : 5716 6294 3671

Mark on parcel

Additional notes

WARNING: our products are of a highly specialised nature and are packaged with the utmost care. The goods delivered are as detailed above. It is essential that all items are checked correctly against this advice note and that they correspond in all respects with your requirements. Any discrepancies should be notified to us immediately. We would advise that all goods are unpacked and handled only by a person qualified to deal with such specialised products to safeguard against injury to the product itself or the purchaser.

Goodfellow

Goodfellow Cambridge Limited
Ermine Business Park, Huntingdon PE29 6WR England
E-mail info@goodfellow.com
Web : www.goodfellow.com
Telephone +44 1480 424 800
Fax +44 1480 424 900

Technische Universität Wien
Stadionallee 2
A-1020 WIEN
AUSTRIA

Your reference
Dated
Our reference LS411293/S D S
AU000341/82
Date 5-Sep-2013

CERTIFICATE OF ANALYSIS

Our reference : LS411293
Your order number : 327
Item number : AU000341/82

Gold : Matrix
Calcium : 3
Iron : 15
Palladium : 9
Platinum : 10
Rhodium : 4
Ruthenium : 3
Sodium : 2
Tin : 4

All impurities in ppm unless otherwise stated.
The analysis was performed on this batch either in the final form or at an earlier stage of manufacture.

Goodfellow

Goodfellow Cambridge Limited
Ermine Business Park, Huntingdon PE29 6WR England
E-mail info@goodfellow.com
Web : www.goodfellow.com
Telephone +44 1480 424 800
Fax +44 1480 424 900

Technische Universität Wien
Stadionallee 2
A-1020 WIEN
AUSTRIA

Your reference
Dated
Our reference LS411293/S D S
CU000745/11
Date 5-Sep-2013

CERTIFICATE OF ANALYSIS

Our reference : LS411293
Your order number : 327
Item number : CU000745/11

Copper	: Matrix
Antimony	: 0.51
Arsenic	: 0.20
Bismuth	: 0.14
Cobalt	: 0.26
Iron	: 3.3
Lead	: 0.21
Nickel	: 0.55
Silicon	: 0.11
Silver	: 7.2
Tantalum	: <1
Tin	: 0.11

All impurities in ppm unless otherwise stated.

The analysis was performed on this batch either in the final form or at an earlier stage of manufacture.

Goodfellow

Goodfellow Cambridge Limited
Ermine Business Park, Huntingdon PE29 6WR England
E-mail info@goodfellow.com
Web : www.goodfellow.com
Telephone +44 1480 424 800
Fax +44 1480 424 900

Technische Universität Wien
Stadionallee 2
A-1020 WIEN
AUSTRIA

Your reference
Dated
Our reference LS411293/S D S
IN000266/34
Date 5-Sep-2013

CERTIFICATE OF ANALYSIS

Our reference : LS411293
Your order number : 327
Item number : IN000266/34

Indium : Matrix
Cadmium : <1
Copper : <1
Iron : <1
Lead : <1
Nickel : <1
Thallium : <1
Tin : <1
Zinc : <1

All impurities in ppm unless otherwise stated.
The analysis was performed on this batch either in the final form or at an earlier stage of manufacture.

Goodfellow

Goodfellow Cambridge Limited
Ermine Business Park, Huntingdon PE29 6WR England
E-mail info@goodfellow.com
Web : www.goodfellow.com
Telephone +44 1480 424 800
Fax +44 1480 424 900

Technische Universität Wien
Stadionallee 2
A-1020 WIEN
AUSTRIA

Your reference	
Dated	
Our reference	LS411293/J V
	NI000605/10
Date	9-Sep-2013

CERTIFICATE OF ANALYSIS

Our reference : LS411293
Your order number : 327
Item number : NI000605/10

Nickel	: Matrix
Aluminium	: 0.7
Iron	: 0.8
Molybdenum	: 2
Silicon	: 0.9

All impurities in ppm unless otherwise stated.
The analysis was performed on this batch either in the final form or at an earlier stage of manufacture.

Goodfellow

Goodfellow Cambridge Limited
Ermine Business Park, Huntingdon PE29 6WR England
E-mail info@goodfellow.com
Web : www.goodfellow.com
Telephone +44 1480 424 800
Fax +44 1480 424 900

Technische Universität Wien
Stadionallee 2
A-1020 WIEN
AUSTRIA

Your reference
Dated
Our reference LS411293/S D S
FE000411/41
Date 5-Sep-2013

CERTIFICATE OF ANALYSIS

Our reference : LS411293
Your order number : 327
Item number : FE000411/41

Iron	: Matrix
Aluminium	: 1.6
Arsenic	: 0.12
Boron	: 2.3
Carbon	: 12
Chromium	: 3.2
Cobalt	: 15
Copper	: 2
Gallium	: 0.29
Germanium	: 5.9
Manganese	: 0.87
Molybdenum	: 0.28
Nickel	: 16
Niobium	: <.1
Phosphorous	: 7.3
Potassium	: 0.23
Silicon	: 36
Sodium	: 0.25
Tantalum	: <10
Titanium	: 0.41
Tungsten	: 0.18
Vanadium	: 0.49
Zinc	: 0.19

All impurities in ppm unless otherwise stated.
The analysis was performed on this batch either in the final form or at an earlier stage of manufacture.

Goodfellow

Goodfellow Cambridge Limited
Ermine Business Park, Huntingdon PE29 6WR England
E-mail info@goodfellow.com
Web : www.goodfellow.com
Telephone +44 1480 424 800
Fax +44 1480 424 900

Technische Universität Wien
Stadionallee 2
A-1020 WIEN
AUSTRIA

Your reference
Dated
Our reference LS411293/S D S
AL000630/20
Date 5-Sep-2013

CERTIFICATE OF ANALYSIS

Our reference : LS411293
Your order number : 327
Item number : AL000630/20

Aluminium : Matrix
Cerium : 0.591
Iron : 1.85
Magnesium : 1.15
Phosphorous: 2.62
Silicon : 1.31

All impurities in ppm unless otherwise stated.
The analysis was performed on this batch either in the final form or at an earlier stage of manufacture.

D Blueprints of the Vertical Cross Section of the Reactor

[H]

WERE 23.05.1996

